https://doi.org/10.1016/j.jclepro.2019.06.224

Investigation of Energy-Saving Azeotropic Dividing Wall Column to Achieve Cleaner Production via Heat Exchanger Network and Heat Pump Technique

Ao Yang[a], Saimeng Jin[a], Weifeng Shen[a,*], Peizhe Cui[b,*], I-Lung Chien[c] and Jingzheng Ren[d]

[a]School of Chemistry and Chemical Engineering, Chongqing University, Chongqing 400044, R. P. China

[b]College of Chemical Engineering, Qingdao University of Science and Technology, 53 Zhengzhou Road, Qingdao, 266042, China

[c]Department of Chemical Engineering, National Taiwan University, Taipei 10617, Taiwan

[d]Department of Industrial and Systems Engineering, The Hong Kong Polytechnic University, Hong Kong SAR, R. P. China

Corresponding author:

Email Address: shenweifeng@cqu.edu.cn (W. Shen) or cpzmagic@qust.edu.cn (P. Cui)

Abstract: A thermally coupled azeotropic dividing wall column (ADWC) process is explored for the separation of industrial wastewater to recycle the organic solvent tert-butanol. Heat pump technology is used to the ADWC process herein to improve the released heat duty quality of the condenser achieving the purpose of energy-saving. A gas preheater before the compressor is then installed in the heat pump assisted ADWC process to increase the temperature of the inlet vapor stream of the compressor that achieves effectively reducing the power and compression ratio of the compressor. To fully utilize the large amount of superheat energy produced in heat pump system via the observation of the temperature-enthalpy and grand composite curve diagrams, a green and sustainable self-heat ADWC (SH-ADWC) separation process is proposed by the combined use of heat exchange network and heat pump techniques. Furthermore, three indexes involving total annual cost (TAC), carbon dioxide emissions, and exergy loss are introduced to evaluate the economic, environmental and thermodynamic performances. The results illustrate that the TAC of the proposed green and sustainable SH-ADWC scheme is significantly reduced by 32.91% with a ten-year payback period compared to that of the existing process. Moreover, carbon dioxide emissions and exergy loss of the SH-ADWC scheme are reduced by 86.43% and 36.72%, respectively. Of note is that the proposed method for the green and sustainable SH-ADWC configuration could be widely extended to other industrial processes to achieve reduction in TAC and sustainable development.

Keywords: Azeotropic dividing wall column; Energy-saving; Heat exchanger network; Heat pump; Distillation

Nomenclature:

ADWC	azeotropic dividing wall column
C%	the carbon content of fuel, kg/kg
CCC	cold composition curve
COM	compressor
COP	coefficient of performance
CO_2	carbon dioxide
CYH	cyclohexane
C_{TBA}	total cost of tert-butanol, US$/year
C_{Energy}	total cost of energy consumption, US$/year
C_{RM}	total cost of raw material, US$/year
C_{WT}	total cost of wastewater treatment, US$/year
DWC	dividing wall column
El	exergy loss, kW
E*x*	exergy, kW
GP-HP-ADWC	heat pump assisted azeotropic dividing wall column with a gas preheater
GCC	grand composite curve
H	enthalpy, kW
HP	heat pump
HP-ADWC	heat pump assisted azeotropic dividing wall column
HEN	heat exchanger network
HCC	hot composition curve
NHV	the net heating value of fuel, kJ/kg
NRTL	non-random two liquid

Q_{CW}	cold utility, kW
Q_{LP}	hot utility, kW
Q_{fuel}	the heat requirement of fuel, kJ
Q_{seq}	energy requirement, kJ
S	entropy, kW
SH-ADWC	self-heat azeotropic dividing wall column
T_{inlet}	inlet temperature, K
T_{outlet}	outlet temperature, K
T-H	temperature-enthalpy
TBA	tert-butanol
T	temperature, K
TAC	total annual cost, US$/year
TCC	total capital cost, US$
TOC	total operating cost, US$/year
TNR	total net revenue, US$/year
T_R	reboiler temperature
T_C	condenser temperature
x	molar composition, mol/mol
α	the molar mass ratio of CO_2 and C
λ_{seq}	latent heat of the steam, kJ/kg
h_{seq}	enthalpy of the steam, kJ/kg
η_C	Carnot efficiency

1. Introduction

Distillation technology has been frequently developed for separating and purifying of mixtures in the chemical industrial due to its advantages in the operation and control (Luyben and Chien, 2011; Sharan et al., 2018). However, major defect of the conventional distillation is required a great deal of energy consumption to achieve the separation task (Kiss and Ignat, 2012). In addition, a large amount of carbon dioxide emissions will cause environmental pollution (Silva et al., 2018; Todd and Baroutian, 2017; Wang et al., 2019b). Therefore, intensified distillation processes must be developed to overcome the above issues achieving the performance of energy-saving, cleaner production and environmental protection (Matsuda et al., 2012; Sharan et al., 2018; Silva et al., 2017).

To achieve the energy-saving, distillation processes with heat integration by changing operating pressure as a technology is explored. For example, a novel pressure-swing extractive distillation configuration for separating acetone/methanol binary minimum-boiling azeotropic mixture is explored (You et al., 2017). The application of heat integration for the extractive distillation process to separate tetrahydrofuran/water mixtures with a lower operational pressure are then investigated (Gu et al., 2018). Design and optimization of ternary extractive distillation for separating acetonitrile/methanol/water is proposed by Wang et al. (2019a) and the calculation illustrates that total annual cost (TAC) of the lower operating pressure scheme can reduce by 47.0% than the operating at atmosphere pressure. Following that, vacuum distillation scheme for low-sulfur biodiesel production is explored by Xie et al. (2019). Furthermore, a novel separation configuration as another energy-saving technology is investigated. For instance, a novel energy-saving extractive distillation with side-stream is studied by Tututi-Avila et al. (2017) for the separation of acetone/methanol mixtures using water as entrainer. Partial thermally coupled and double side-streams ternary extractive distillation sequences for acetonitrile/benzene/methanol separation are explored by Wang et al. (2018). In summary, energy consumption and carbon dioxide emissions of the process could be reduce via the intensified distillation configuration or heat integration scheme.

To further reduce the energy consumption, fully thermally coupled dividing wall column (denoted as DWC) process is extensively explored. Zhou et al. (2018) proposed a DWC sequence for organic waste treatment and recovery in the synthesis of nylon. Kiss and Ignat (2012) reported that the steam cost of the DWC scheme can save up to 30% than the double-column separation sequence. Besides, DWC can also be applied to implement other processes (e.g., azeotropic, extractive and reactive distillations) with a dividing wall located at the bottom, top and middle of the operating unit, respectively. For example, Wu et al. (2014) proposed an energy-saving azeotropic-DWC (ADWC) separation configuration for heterogeneous azeotropic distillation. Yu et al. (2015) investigated the implementation of ethanol dehydration by employing ADWC. Wu et al. (2013) explored the energy-efficient potential of the extractive-DWC for heterogeneous distillation processes. The application of extractive-DWC for ethane recovery process is then studied (Tavan et al., 2014). Yang et al. (2018) studied the separation of ternary heterogeneous mixtures methanol/toluene/water with multi-azeotrope system through using extractive-DWC with a side decanter configuration. Synthesis of tert-amyl methyl ether through combination the DWC with reaction distillation and pressure-swing configuration is proposed by Yang et al. (2017). Reactive-DWC scheme for the synthesis of triethyl citrate using multi-objective criteria is reported by Santaella et al. (2017). The above results show that the energy consumption of the DWC configuration could be further reduced than that of the conventional sequence.

DWCs separation technology can provide a huge potential to effectively reduce the steam consumption. However, the heat duty of condenser has not been effectively utilized in the DWC sequence. Hence, heat pump (HP) technology is employed to improve the released heat duty quality of the condenser to conform to the heat demand of the reboiler and is mainly utilized to reduce energy required when the difference of temperature between the top and bottom of column is small (Kumar et al., 2013; Luo et al., 2015; Modla and Lang, 2015). HP technique can be easily applied to existing processes because they can be installed externally and require little change to the existing designs (Olujić et al., 2006). For example, Long et al. (2015) proposed a novel self-heat DWC to improve the thermodynamic efficiency and production capacity of the column and the calculations illustrate that the self-heat process can effectively reduce the operating cost. Li et al. (2016) explored the energy-saving of three HP configurations for the ADWC and the computational results show that the improved design configuration saves a TAC by 32.22% and carbon dioxide (CO_2) emissions by 63.79%. Xu et al. (2017) reported an approach to design intensified configurations involving the HP assisted DWC at the side product stage and they illustrate that intermediate reboiler-side condenser HP assisted DWC scheme can reduce 8.57% of TAC. An improved different pressure thermally coupled reactive-DWC for the synthesis of diethyl carbonate is proposed in our recently work (Yang et al., 2019b) by using HP technique and the calculation illustrates that the TAC of the proposed scheme could be reduced by 20.52%. In summary, better environmental and economic benefits can be achieved in the DWC scheme because of the latent heat of vaporization in top vapor stream is effectively utilized via the HP technology.

A mount of sensible heat in the hot and cold streams are not well used because of the HP is applied in the distillation process. In order to comprehensively and effectively utilize the heat duty of cold and hot streams in the process, heat exchanger network (HEN) and pinch analysis are used to effectively decrease the requirements of steam and cooling water (Wang et al., 2009). A whole process with heat integration implementing HP is reported by Yang et al. (2016). In the proposed design, the steam and cooling water requirements are reduced by 61.5% and 20.6%, respectively, compared to the conventional process. Next, the HEN is employed to the heat integration design in the biodiesel production through the reactive distillation (Poddar et al., 2017) and they provided evidences that the operating cost of the heat-integrated process is significantly reduced compared with the referenced process. Based on the above studies, Xia et al. (2017) proposed a heat pump assisted pressure-swing distillation scheme with HEN matching and they demonstrated that proposed process reduces TAC by 36.65% and 5.18% compared with the conventional and full heat integrated designs, respectively. In a few words, the application of HEN can be employed to find a scheme with small energy consumption, TAC and CO_2 emissions.

To the best of our knowledge, few studies have reported the application of both HEN and HP technologies to the ADWC process. As a consequence, in this work, a novel green and sustainable self-heat ADWC (SH-ADWC) configuration is proposed by combining HP and HEN techniques for separating binary azeotropic mixtures tert-butanol (TBA)/water to achieve the purpose of cleaner production (i.e., energy-saving, reduction of CO_2 emissions and enhancing of thermodynamic efficiency). A conventional ADWC scheme is firstly simulated by the Aspen Plus simulator as a basic case. Following that, the ADWC with feed preheating (ADWC-FP) scheme is proposed to reduce the energy consumption of reboiler. HP assisted ADWC (HP-ADWC2) configuration is then proposed to further achieve saving-energy performance. After that, a gas preheater before the compressor is installed to make further efforts for reducing the power of the compressor. Finally, the HEN is also applied to achieve the optimal heat matching in the proposed green and sustainable SH-ADWC process.

2. Methodology

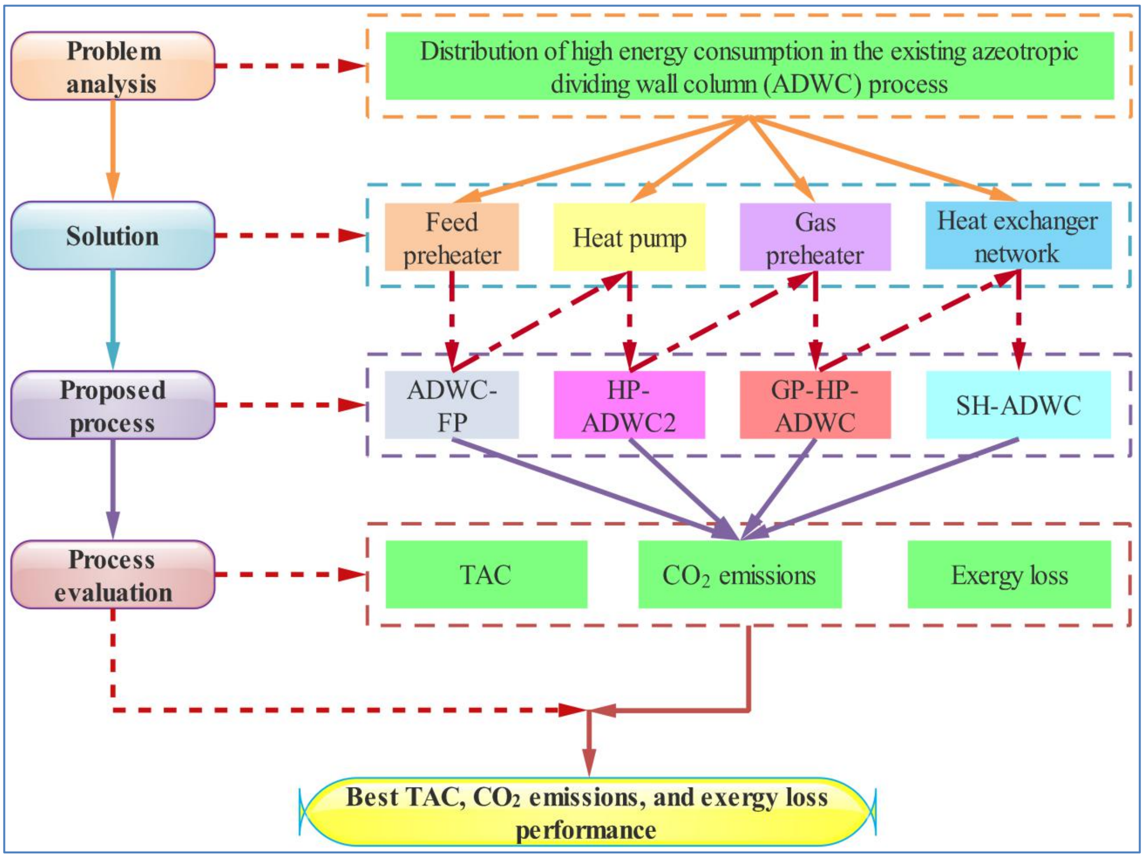

Fig. 1. Proposed framework of the SH-ADWC process design and evaluation

A systematic method is proposed for the design of the TBA dehydration process by combining the HP and HEN technologies into the ADWC scheme, as described in Fig. 1. In the first step, energy analysis of the existing process is carried out to search suitable alternative solutions. Next, four solutions are found to effectively reduce the energy consumption or improve the released heat duty quality of the condenser. In the solution step, feed preheater is used to heat the feed streams reducing the reboiler duty. Following that, HP is installed to further reduce the energy consumption. A gas preheater before the compressor is added to effectively decrease the compressor ratio and power. Heat exchanger network is used to match the latent heat of vaporization and sensible for hot and cold stream achieving optimal design. To validate the proposed solutions, four alternative configurations combining feed preheater, heat pump, a gas preheater for the compressor and heat exchanger network with ADWC process (i.e., ADWC-FP, HP-ADWC2, GP-HP-ADWC and

SH-ADWC) are implemented via the Aspen Plus. Finally, three indexes involving TAC, CO_2 emission and exergy loss are introduced to evaluate TBA dehydration process by alternative configurations and the existing process.

2.1 Existing azeotropic dividing wall column scheme

2.1.1 Azeotropic dividing wall column scheme

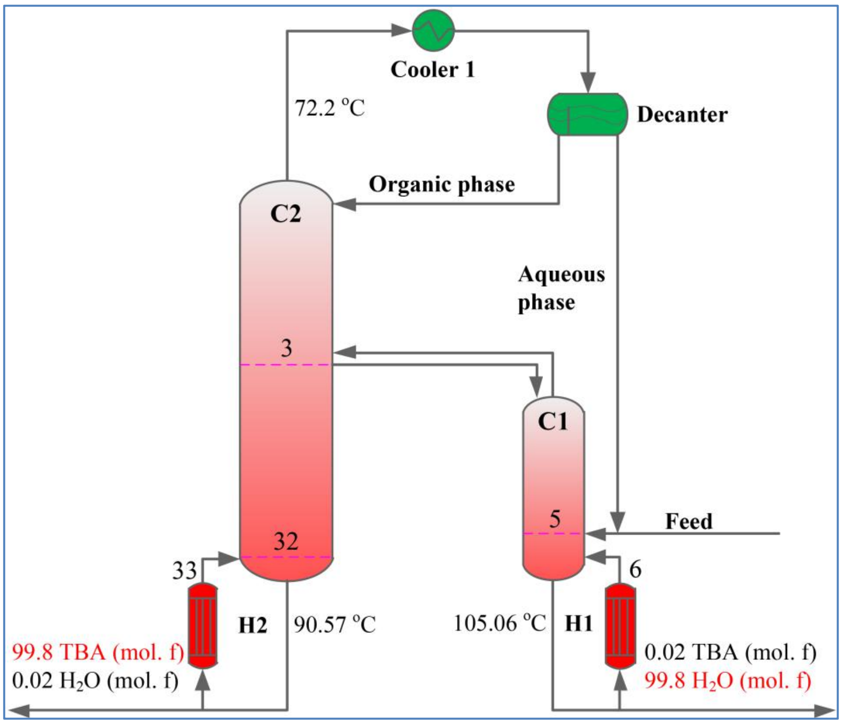

Fig. 2. Existing ADWC scheme for TBA dehydration

In this work, the existing ADWC scheme for separating binary azeotropic system TBA/water is proposed by Luyben (2016). The existing ADWC scheme for TBA dehydration process is illustrated in Fig. 2. The fresh feed and the aqueous stream from the decanter is mixed and then fed into the column C2. High-purity water with 99.8 mol% is obtained at the bottom stream of column C1 while the top vapor stream and organic stream are sent to the middle and top sections of column C2. High-purity TBA with 99.8 mol% is obtained at the bottom of column C2 while the top vapor stream is condensed to the decanter. Finally, aqueous and organic phases are obtained via the decanter.

2.1.2 Evaluation the feasibility of the HP assisted ADWC

Pleşu et al. (2014) proposed a simple criterion coefficient of performance (denoted as COP) defining as in Eq. 1 to effectively evaluate the feasibility of a HP system.

$$\mathrm{COP} = \frac{Q}{W} = \frac{1}{\eta_C} = \frac{T_\mathrm{C}}{T_\mathrm{R} - T_\mathrm{C}} \tag{1}$$

where the reboiler duty is represented as Q, the requirement work of the compressor is denoted as W, Carnot efficiency is represented as η_C, the reboiler temperature is represented as T_R (K) and the condenser temperature is denoted as T_C (K).

From the study of Luyben (2016) in Fig. 2, the temperature of the top vapor stream is 72.2 ^{o}C (345.35 K) while the temperatures of left and right reboilers are 105.06 ^{o}C and 90.57 ^{o}C (378.21 K and 363.72 K), respectively. The calculation COPs of C1 and C2 are 10.51 and 18.80 (both higher than 10), respectively, indicating that the application of HP in C1 and C2 (or ADWC) process for separating TBA/water system is very favorable.

2.1.3 Energy analysis via the temperature-enthalpy diagram

In generally, the utility requirements of the chemical industrial process can be well represented via the temperature-enthalpy (T-H) diagram (Yang et al., 2016). The overall hot and cold requirements are observed through the hot composition curve (denoted as HCC) and cold composition curve (abbreviated as CCC) in the T-H diagram (Poddar et al., 2017). The recovery heat of the process could be represented in the overlap region of HCC and CCC. In addition, the cooling water and steam requirements are the displacements of the CCC and HCC (Xia et al., 2017).

2.2 Four proposed alternative configurations

2.2.1 ADWC with feed preheating (ADWC-FP)

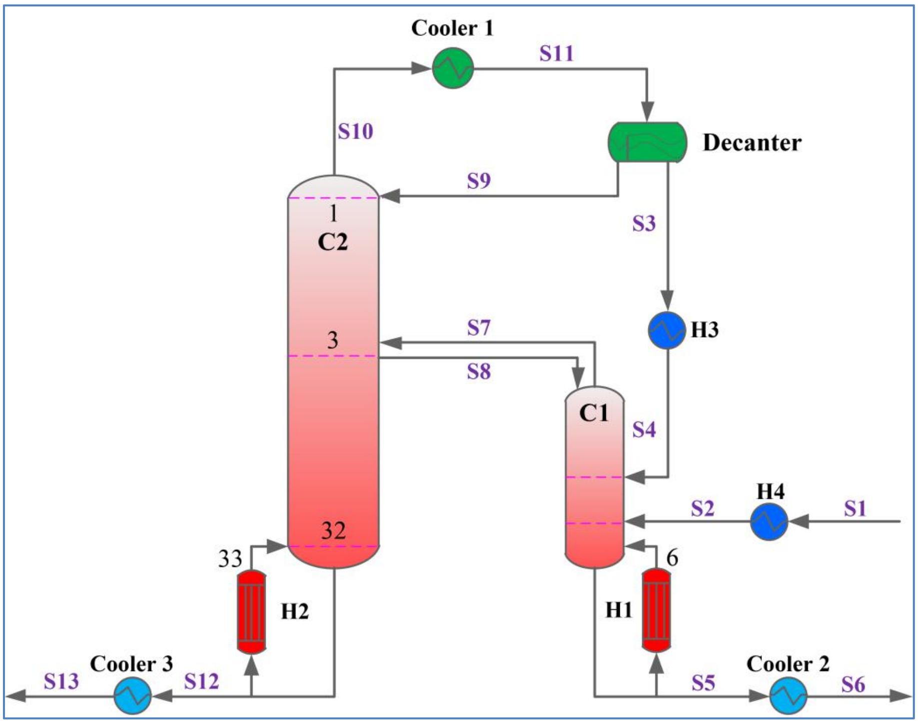

Fig. 3. Proposed alternative configuration ADWC-FP for TBA dehydration

Fig. 3 illustrates the proposed alternative configuration ADWC with feed preheating (ADWC-FP) for TBA dehydration. To reduce the energy consumption of the ADWC scheme, two feed stream (i.e., S3 and S4) should be preheated to decrease the reboiler duty of column C1 (Xia et al., 2017). Compared with ADWC, the power consumption of compressor can be reduced when the HP is applied in the ADWC-FP. Following the suggestion of Xia et al. (2017), two product streams S5 and S12 should be cooled to 40 °C. Of note is that the feed stream S9 is not preheated because of this stream is fed to the first stage. Furthermore, the feed locations of S2 and S4 should be optimized because of the thermal state of the feed has been changed.

2.2.2 HP assisted ADWC (HP-ADWC2)

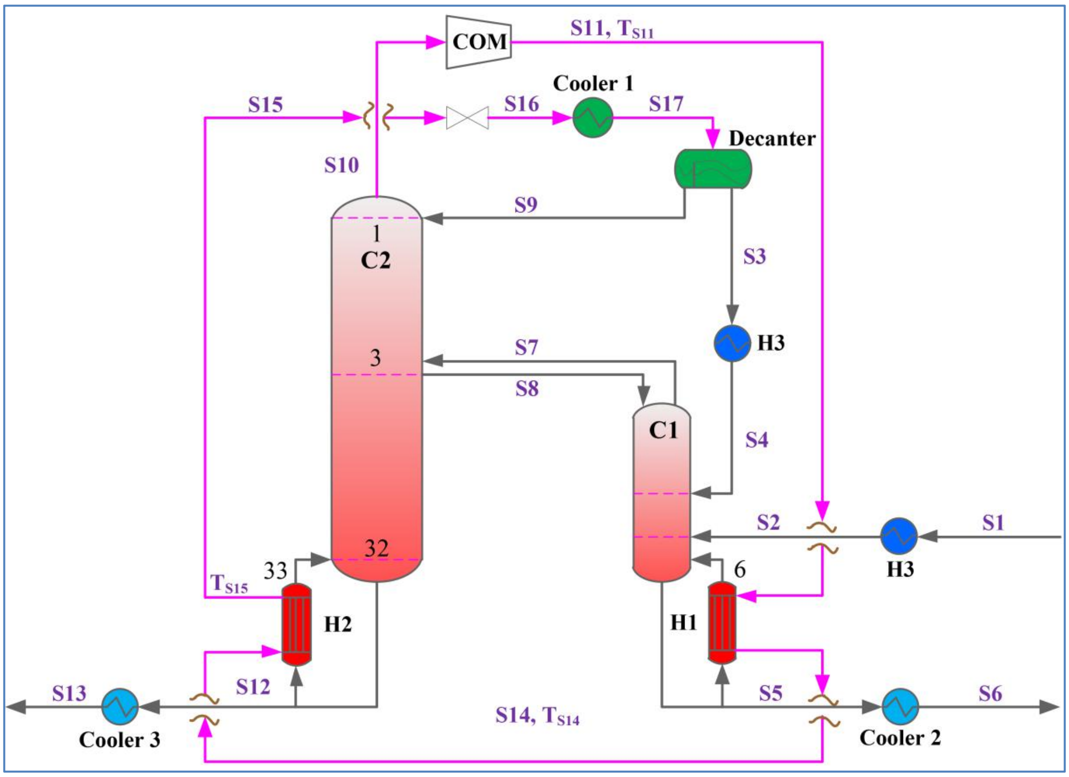

Fig. 4. Proposed alternative configuration HP-ADWC2 for TBA dehydration

The proposed alternative configuration HP assisted ADWC (HP-ADWC2) for TBA dehydration is displayed in Fig. 4. To effectively utilize the latent heat of vaporization in top vapor stream of column C2, a compressor is installed at the top of the column C2. The top vapor stream of the column C2 is compressed to a high temperature to provide heat duty for reboilers H1 and H2. In the simulation process, a new design specification is set by varying the outlet pressure of compressor to satisfy the T_{S15}-$T_{R2} \geq 5$ °C and T_{S14}-$T_{R1} \geq 5$ °C (T_{S15} and T_{S14} represent the temperature of S15 and S14 streams). However, the condenser duty is lower than the sum of heat duty for H1 and H2 according to the study of Luyben (2016). To achieve the heat exchanger, a higher temperature of compressed stream is required, which may cause a greater compression ratio for the compressor. Therefore, a more energy-saving scheme should be proposed to further reduce the power consumption of compressor.

2.2.3 A gas preheater is installed before the compressor for the HP-ADWC2 (GP-HP-ADWC)

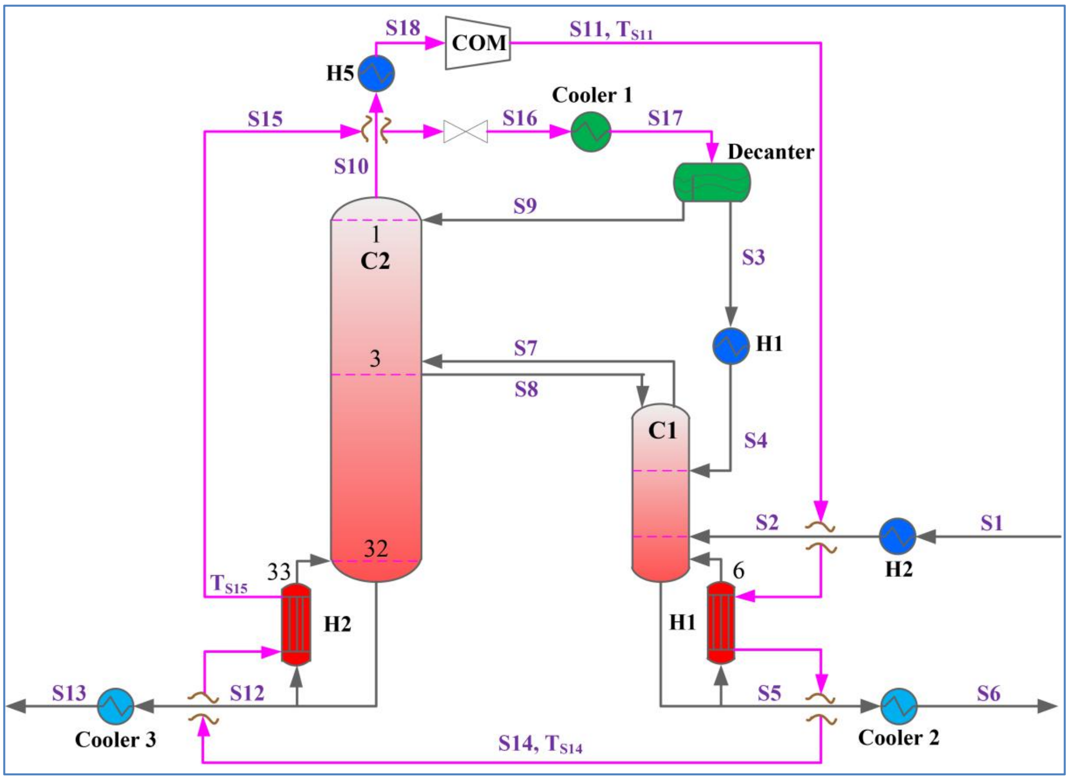

Fig. 5. Proposed alternative configuration GP-HP-ADWC for TBA dehydration

Following the suggestion of Li et al. (2016), a gas preheater before the compressor is installed in the HP-ADWC2 scheme (denoted as GP-HP-ADWC) as illustrated in Fig. 5, which could effectively reduce the power of the compressor. Compared with the HP-ADWC scheme, the compressor ratio (or outlet pressure) of the GP-HP-ADWC with a higher temperature of compressor inlet may be effectively reduced. The temperature of stream S18 should be optimized because of it will affect the power of compressor (W) and the outlet temperature of compressed stream (T_{S11}). It is worth noting that a heat input is needed for the gas preheater H5. In addition, the sensible heat of stream S15 and product streams S5 and S12 are not effectively utilized. The optimal heat matching will be shown in the below section 2.2.4.

2.2.4 Self-heat ADWC (SH-ADWC) scheme

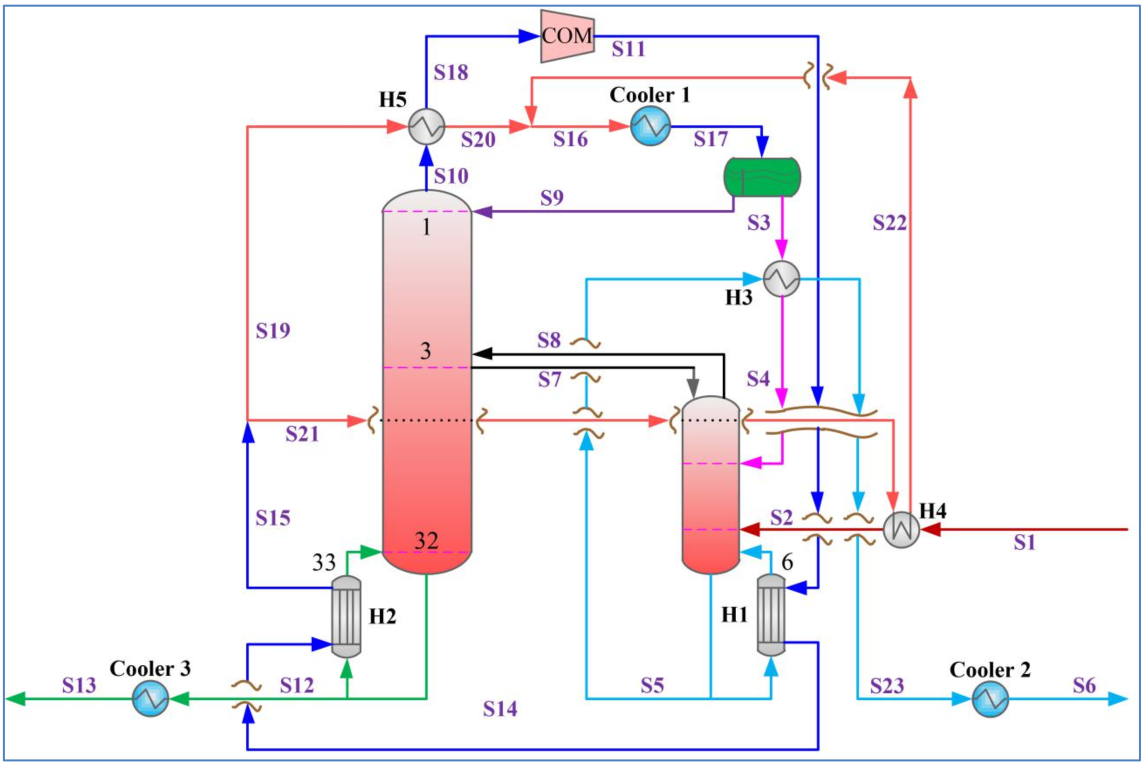

Fig. 6. Proposed alternative configuration SH-ADWC for TBA dehydration

Following the suggestion of Liu et al. (2018) and Wang et al. (2009), heat exchanger network (HEN) could be used to match the hot and cold stream achieving the minimum energy consumption. To achieve the optimal and reasonable matching, pinch analysis is used (Klemeš et al., 2018; Walmsley et al., 2018), which is carried out in the Aspen Energy Analyzer. Fig. 6 demonstrates a conceptual design flowsheet of the optimal hot and cold stream matching. The heat duties of feed preheater (H1 and H2), reboiler 1 (H3), reboiler 2 (H4), gas preheater (H5), and coolers (cooler 1-3) and minimum pinch point temperature should be determined in section 3.2.4. Furthermore, the energy-saving of the SH-ADWC should be re-evaluated because of more capital investment is needed compared with the GP-HP-ADWC.

2.3 Economic, environmental and thermodynamic efficiency evaluations

In this investigation, three criteria (i.e., TAC, carbon dioxide emissions and exergy loss) are used to evaluate the economic, environmental and thermodynamic efficiency of the existing and proposed schemes.

2.3.1 Economic evaluation

TAC proposed by Douglas (1988) is introduced to assess the economics of the existing and the intensified designs, which consists of the total capital cost (TCC) and total operating cost (TOC). Computational formula of the TAC is illustrated as follow,

$$\text{TAC [US\$/year]} = \text{TCC} / \text{payback} + \text{TOC} \tag{2}$$

TCC involves the capital costs of shell, tray, decanter, condensers, reboilers, heat exchangers, and compressor.

The shell and tray costs of the column are calculated as follow,

$$\text{shell cost of column [US\$]} = (\text{M\&S}) / 280 \times D^{1.066} \times H^{0.802} \times C_{\text{SC}} \tag{3}$$

$$\text{tray cost of column [US\$]} = (\text{M\&S}) / 280 \times 97.243 \times D^{1.55} \times H \times F_{\text{C}} \tag{4}$$

where Marshall and Swift index (M&S) is assumed as 1468.6 to the HP system (Feng et al., 2018); H [m] and D [m] represent the height and the diameter; coefficients of the shell cost for column and decanter (C_{SC}) is 3919.32 (Olujić et al., 2006); correction factor of the tray cost (F_{C}) is determined as 1.4 (Olujić et al., 2006).

Capital costs for the reboiler, condenser, and heat exchanger are obtained as follow,

$$\text{heat exchanger cost [US\$]} = (\text{M\&S}) / 280 \times A^{0.65} \times C_{\text{H}} \tag{5}$$

where A (m^2) denotes the area of reboiler, condenser, and heat exchanger; coefficients of the kettle reboiler, condenser, and heat exchanger (C_{H}) are 1775.26, 1609.13, and 1799.00, respectively (Olujić et al., 2006).

Calculations of area and heat transfer temperature difference for the reboiler and heat exchanger are displayed as follow,

$$A_{\mathrm{R}}[\mathrm{m}^2]=\frac{Q_{\mathrm{R}}}{(\Delta T_{\mathrm{R}}\times U_{\mathrm{R}})} \tag{6}$$

$$\Delta T_{\mathrm{R}}\ [\mathrm{K}]=160-T_{\mathrm{R}} \tag{7}$$

$$\Delta T_{\mathrm{R}}\ [\mathrm{K}]=\frac{(T_{\mathrm{hin}}-T_{\mathrm{cout}})-(T_{\mathrm{hout}}-T_{\mathrm{cin}})}{\ln(\frac{T_{\mathrm{hin}}-T_{\mathrm{cout}}}{T_{\mathrm{hout}}-T_{\mathrm{cin}}})} \tag{8}$$

where A_R [m^2] represents the area of the reboiler and heat exchanger; Q_R is the reboiler duty; U_R = 568 W/m^2/K is the heat transfer coefficient of the reboiler while U_R is 210 W/m^2/K for the gas preheater (Luyben, 2012); T_R [K] are the reboiler temperature of the compressed vapor stream; ΔT_R [K] in Eq. 7 denotes the heat transfer temperature difference of reboiler when the low pressure steam is used; ΔT_R [K] in Eq. 8 denotes the heat transfer temperature difference of heat exchanger while the reboiler input is provided via the compressed vapor stream; the inlet and outlet temperatures of the high temperature stream denote as T_{hin} and T_{hout}, respectively; the inlet and outlet temperature of the low temperature stream represent T_{cin} and T_{cout}, respectively.

Calculations of area and heat transfer temperature difference for the condenser are shown as follow,

$$A_{\mathrm{C}}\ [\mathrm{m}^2]=\frac{Q_{\mathrm{C}}}{(\Delta T_{\mathrm{C}}\times U_{\mathrm{C}})} \tag{9}$$

$$\Delta T_{\mathrm{C}}\ [\mathrm{K}]=\frac{(T_{\mathrm{hin}}-T_{\mathrm{cout}})-(T_{\mathrm{hout}}-T_{\mathrm{cin}})}{\ln(\frac{T_{\mathrm{hin}}-T_{\mathrm{cout}}}{T_{\mathrm{hout}}-T_{\mathrm{cin}}})} \tag{10}$$

where A_C [m^2] is the area of the condenser; Q_C [kW] is the condenser duty; U_C = 852 W/m^2/K is the heat transfer coefficient of the condenser (Luyben, 2012); ΔT_C is the logarithmic mean temperature difference, which is calculated via the Eq. 10; T_{cin} and T_{cout} are 30 and 40 °C while the cooling water is used (Modla and Lang, 2013; Premkumar and Rangaiah, 2009).

The capital cost and volume of the decanter could be obtained from the Eqs. 11 and 12 (Turton et al., 2008).

$$\text{decanter cost [US\$]} = (\text{M\&S})/280 \times D_{\text{d}}^{1.066} \times H_{\text{d}}^{0.802} \times C_{\text{SC}} \tag{11}$$

$$V_{\text{d}}\ [\text{m}^3] = F_{\text{V}} \times 2 \times 10/60 = \frac{\pi D_{\text{d}}^2}{4} \times H_{\text{d}} \tag{12}$$

where the height and the diameter of the decanter are abbreviated as D_d (m) and H_d (m); V_d [m^3] is the volume of the decanter. Herein, the ratio of the H_d and D_d is assumed as 2 (Luyben and Chien, 2011).

Calculation of the capital cost for the compressor is illustrated in Eq. 13.

$$\text{capital cost of compressor [US\$]} = (\text{M\&S})/280 \times 2047.24 \times \left[W/(0.9 \times 0.8)\right]^{0.82} \tag{13}$$

TOC includes the operating cost of steam, cooling and electricity, which could be calculated via the Eqs. 14-16.

$$\text{total steam cost [US\$/year]} = C_{\text{S}} \times Q_{\text{R}} \times 7200 \tag{14}$$

$$\text{total cooling water cost [US\$/year]} = C_{\text{W}} \times Q_{\text{C}} \times 7200 \tag{15}$$

$$\text{total electricity cost [US\$/year]} = C_{\text{E}} \times W/(0.9 \times 0.8) \times 7200 \tag{16}$$

where C_S (13.28 US$/GJ), C_W (0.345 US$/GJ), and C_E (16.8 US$/GJ) are the cost of steam, cooling water, and electricity, respectively (Yang et al., 2019b); 7200 h/year is determined as operating time.

Total net revenue (TNR, US$) of the existing and the proposed schemes could be calculated via the Eq. 17 (Silva et al., 2017).

$$\text{total net revenue [US\$/year]} = C_{\text{TBA}} - C_{\text{Energy}} - C_{\text{RM}} - C_{\text{WT}} - \text{TCC}/\text{payback period} \tag{17}$$

where C_{TBA}, C_{Energy}, C_{RM}, and C_{WW} are respectively the total cost of tert-butanol, energy consumption, and raw material wastewater treatment. Prices used in the net revenue analysis are illustrated in Table 1.

Table 1

Product and energy costs for the *tert*-butanol dehydration process.

Product	Price	Units	Reference
Tert-butanol	1000	US$/t	(PHC, 2016)
Raw material	300	US$/t	Information provided by specialists
Low pressure steam	13.28	US$/GJ	(Yang et al., 2019b)
Cooling water	0.345	US$/GJ	(Luyben, 2012; Yang et al., 2019a)
Electricity	16.8	US$/GJ	(Yang et al., 2019b)
Wastewater treatment	1.20	US$/t	(Kim et al., 2009)

Although HP system has a satisfactory performance to reduce the operating cost, it is hard to realize economic benefits in a short investment recovery period. Therefore, ten-year of payback period is determined to observe the energy-saving effect (Yang et al., 2019b).

2.3.2 Carbon dioxide emissions evaluation

CO_2 emission is used to evaluate the environment benefits of HP assisted distillation process (You et al., 2016) and it has been applied to assess the sustainability of the triple-column extractive distillation process (Zhao et al., 2018). Herein, the CO_2 emission is introduced to assess the environment and sustainability of the basic process and proposed processes. However, the calculation of CO_2 emissions is a complex issue due to the energy required for the reboiler could be produced from the different raw materials heavy fuel oil, natural gas, or coal. Therefore, Gadalla et al. (2006) and Tavan et al. (2014) proposed a simplified calculation model of CO_2 emissions in Eq. 2 for the distillation system.

$$\mathrm{CO_2\ emissions} = \left(\frac{Q_{\mathrm{fuel}}}{\mathrm{NHV}}\right) \times \left(\frac{\mathrm{C\%}}{100}\right)\alpha \tag{18}$$

where the molar mass ratio of CO_2 and C (α) is 3.67, the net heating value (denoted as NHV) is 39771 kJ/kg, and C% = 86.5 kg/kg is the carbon content of fuel. The heat requirement of fuel (Q_{fuel}) is calculated as follows,

$$Q_{\mathrm{fuel}} = \frac{Q_{\mathrm{seq}}}{\lambda_{\mathrm{seq}}} \times (h_{\mathrm{seq}} - 419) \times \left(\frac{T_{\mathrm{F}} - T_0}{T_{\mathrm{F}} - T_{\mathrm{S}}}\right) \tag{19}$$

where energy requirements in kJ and latent heat and enthalpy in kJ/kg of the steam are denoted as λ_{seq}, h_{seq} and Q_{seq}, respectively. T_F = 2073.15 K is the flame temperature, T_S = 433.15 K is the stack temperature, and the ambient temperature T_0 is 298.15 K. Following the suggestion of Waheed et al. (2014), CO_2 emission of the compressor is 184 kg/h while the power requirements of a compressor are 1000 kW.

2.3.3 Thermodynamic efficiency evaluation

To evaluate the proposed process, the energy efficiency is another significant indicator. For a given system, the exergy loss (El) is defined as Eq. 20, which exhibits the difference value between total input and output of exergy (Sun et al., 2013).

$$\mathrm{El} = \sum \mathrm{E}x_{\mathrm{input}} - \sum \mathrm{E}x_{\mathrm{output}} \tag{20}$$

Exergy (Ex) is calculated for a given specified system by the enthalpy (H) and entropy (S), which is illustrated in Eq. 21 as follow,

$$\mathrm{E}x = (\mathrm{H} - \mathrm{H}_0) - \mathrm{T}_0 \cdot (\mathrm{S} - \mathrm{S}_0) \tag{21}$$

where the enthalpy difference between the system and the reference state is denoted as $H-H_0$, the $S-S_0$ illustrates the entropy difference between the system and the reference state, and the T_0 =298.15 K is the reference temperature.

3. Computational studies

In the real plant, TBA is always obtained from the direct hydration of isobutene in a reactive distillation process (Lei et al., 2009). Following that, downstream azeotropic mixture (i.e., TBA and water) of the reactive distillation is explored by Yu et al. (2015) to obtain the high-purity of TBA. Next, Luyben (2016) and Chen et al. (2019) investigated the heterogeneous azeotropic distillation to separate TBA/water while an energy-saving extractive distillation in vacuum for the separation of

TBA/water binary azeotropes (see Fig. A1) is proposed by Lo and Chien (2017). In this work, the proposed alternatives configurations are studied based on the heterogeneous heat pump assisted ADWC (also denoted as HP-ADWC1) process by Luyben (2016) due to its advantage in operation.

3.1 Existing ADWC scheme

3.1.1 Residue curve maps

In the ADWC process, the vapor-liquid and liquid-liquid equilibriums of the ternary azeotropic system TBA/water/cyclohexane (CYH) could be well described via the built-in non-random two liquid (NRTL) model (Chen et al., 2019; Luyben, 2016; Yu et al., 2015) of the Aspen Plus while all interaction parameters are summarized in Table 2.

Table 2

Interaction parameters of the NRTL model for the azeotropic distillation system.

Component i	TBA	TBA	Water
Component j	Water	CYH	CYH
Temperature units	ºC	ºC	ºC
A_{ij}	-0.6868	-1.3739	13.1428
A_{ji}	7.0893	1.0691	-10.4585
B_{ij}	203.4190	559.5210	-1066.9800
B_{ji}	-1372.3800	245.1070	4954.9000
C_{ij}	0.3000	0.4700	0.2000

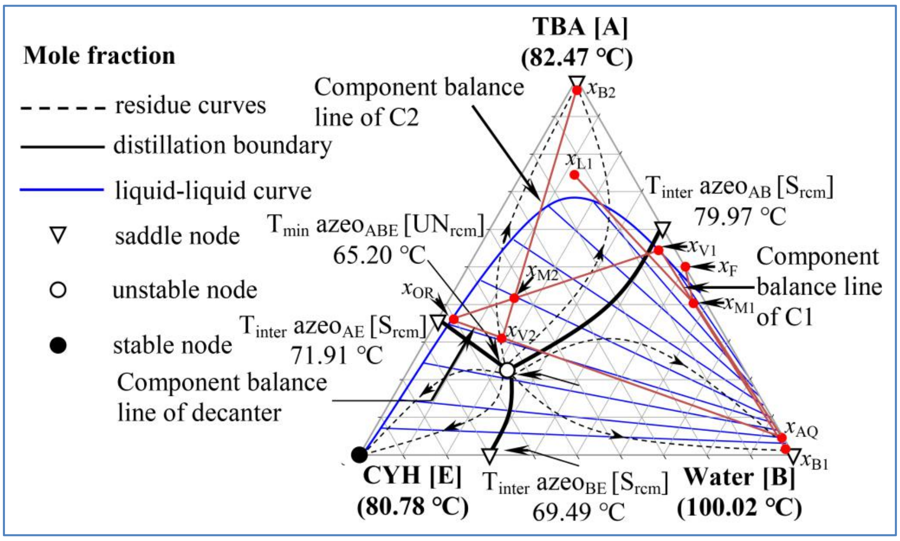

Fig. 7. Residue curve maps and material balance lines for TBA/water system using entrainer CYH

Residue curve maps and material balance lines for TBA/water/CYH system are illustrated in Fig. 7. It is found that three additional azeotropes are formed while the entrainer CYH is added into the TBA/water system. A ternary TBA/water/CYH minimum azeotrope point is located in heterogeneous ranges with an azeotropic temperature of 65.2 °C. Another two azeotropes TBA/CYH and CYH/water are also formed with azeotropic temperatures of 71.9 °C and 69.5 °C, respectively.

The fresh feed (x_F), aqueous phase (x_{AQ}) and liquid sidestream (x_{L1}) are mixed at x_{M1} point and then is separated at a close TBA/water binary azeotropic mixture with a composition x_{V1} and a high purity of water with a composition x_{B1} in the column C1. Following that, the organic phase (x_{OR}) and the top vapor stream x_{V1} of column C1 is mixed at x_{M2} point. A ternary azeotropic mixture (x_{V2}) and a high purity of TBA with a composition x_{B2} are obtained based on the lever rule of the C2. The top vapor stream of the C2, x_{V2}, is cooled to liquid and then it is separated into aqueous and organic phases (i.e., x_{AQ} and x_{OR}) via a decanter.

3.1.2 Process design

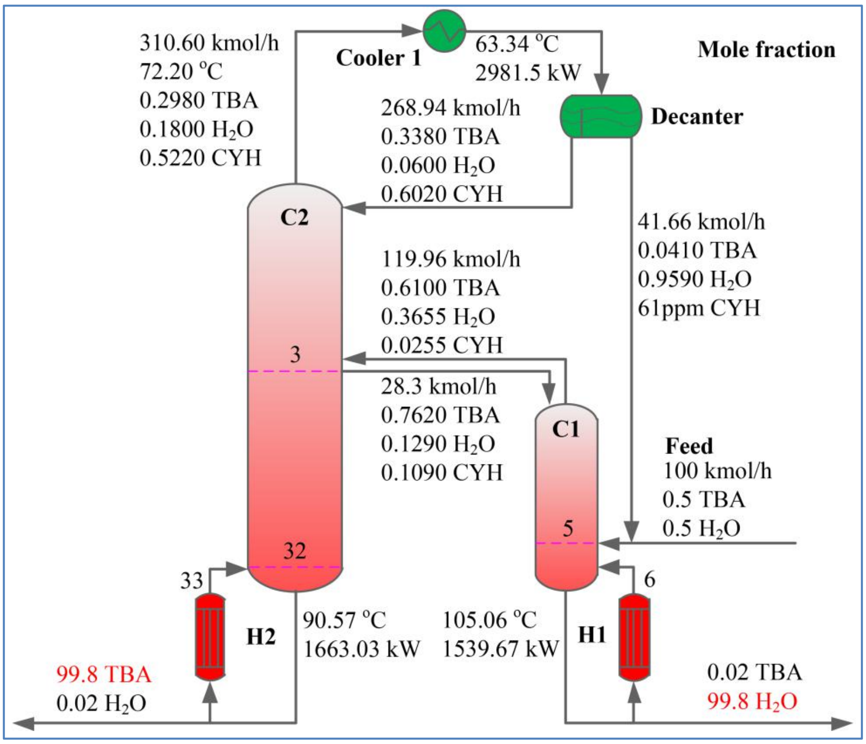

Fig. 8. Scheme of the existing ADWC with detailed parameters by Luyben (2016)

Fig. 8 illustrates the modified ADWC process without heat pump for separating TBA/water azeotropic system by Luyben (2016) while the modified heat pump assisted ADWC (HP-ADWC1) process is illustrated in Fig. A2. Total theoretical stages of two columns C1 and C2 are 6 and 33, respectively. Besides, two columns are both operated at atmospheric pressure while the per tray pressure drop is 0.7 kPa. The aqueous phase and fresh feed are mixed and fed to the column C1, where the mixed stream is separated into a high-purity water in the bottom stream and a ternary azeotropic mixture in the top vapor stream. Following which, the top vapor of column C1 and the organic phase stream are fed to the middle and top section of the C2, respectively. A high-purity of TBA with 99.8 mol% and a ternary azeotropic point TBA/water/CYH mixture are obtained in the column C1 based on the lever rules. The 99.8 mol% of water is obtained at bottom stream of C2. The reboiler duties of columns C1 and C2 are 1539.67 kW and 1663.03 kW, respectively.

3.2 Proposed alternative configurations for TBA dehydration

3.2.1 ADWC with feed preheating (ADWC-FP) scheme

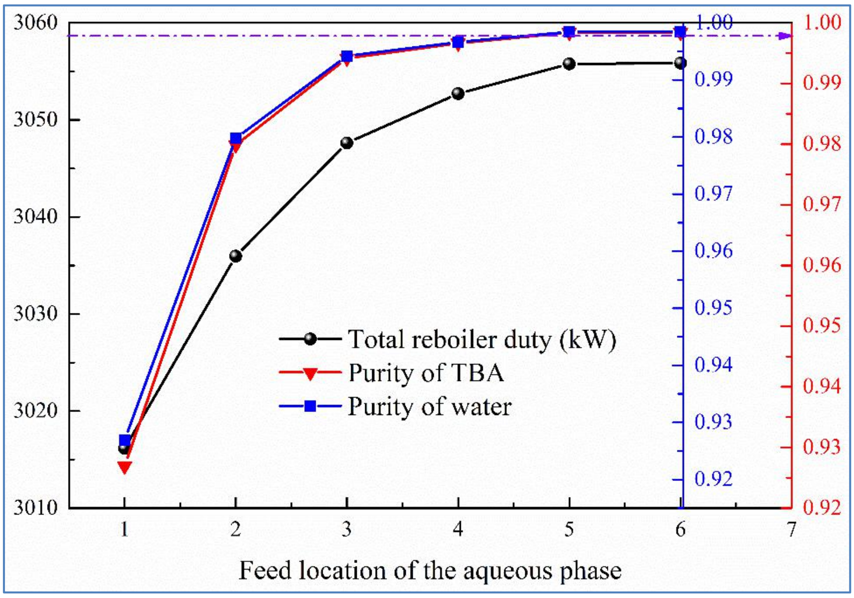

Fig. 9. Effect of the feed location of aqueous phase on total reboiler duty

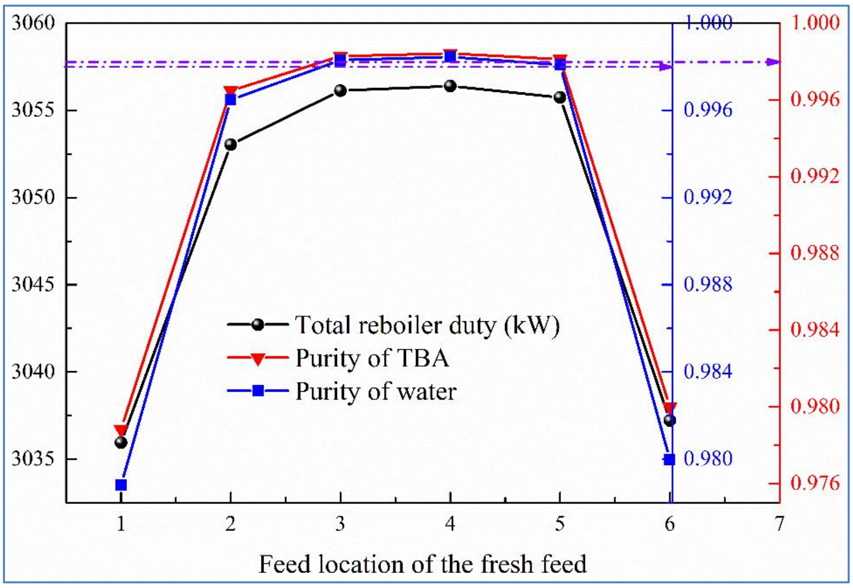

Fig. 10. Effect of the feed location of fresh feed on total reboiler duty

Feed locations of the ADWC-FP scheme is optimized with the total reboiler duty as objective function. The optimizations of feed locations of aqueous phase and fresh feed are illustrated in Figs. 9 and 10, respectively. To achieve the specification products purities with minimum total reboiler duty, the fifth stage is determined as a feed location for aqueous phase and fresh feed.

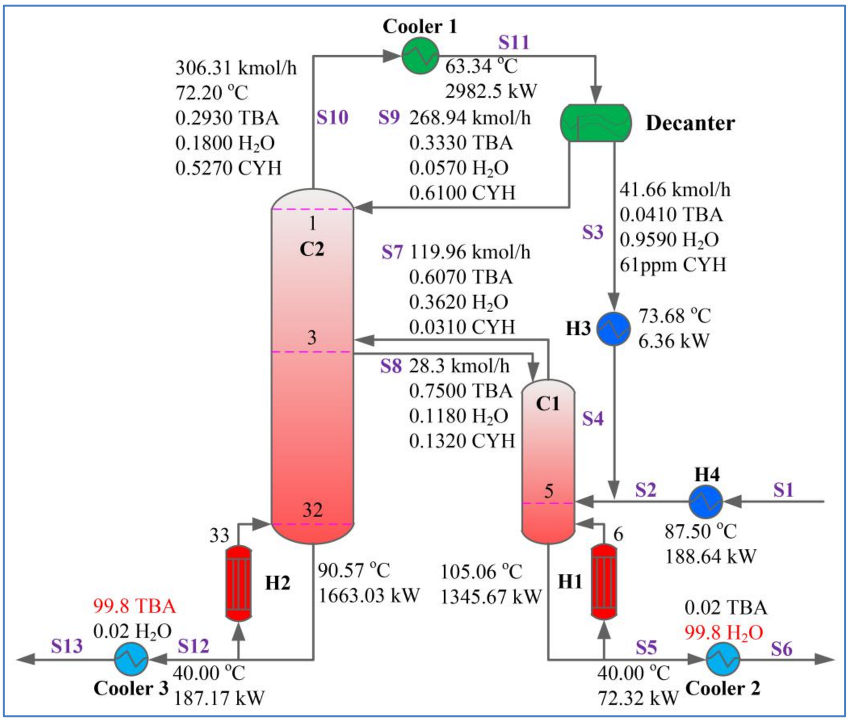

Fig. 11. Flowchart of the ADWC with feed preheating

Fig. 11 shows the ADWC-FP scheme for the separation of TBA/water system by using CYH as a heterogeneous entrainer. The aqueous phase (S3) and fresh feed are preheated at 73.68 ºC and 87.50 ºC via the preheaters 1 and 2 (H3 and H4), respectively. Reboiler duty of column C2 (H2) is 1663.03 kW while 1345.67 kW of H1 in ADWC-FP is obtained compared with the 1539.67 kW of the existing process, which is consistent with the assumptions in Section 2.2.1. Finally, the product streams S12 and S5 are cooled at 40 ºC via the coolers 2 and 3, respectively. The condensation required in coolers 2 and 3 are 187.17 and 72.32 kW, respectively.

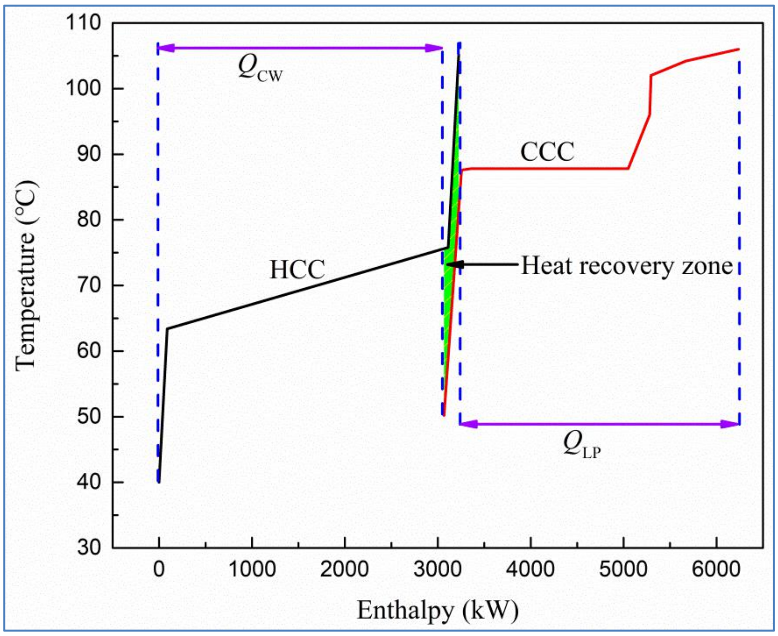

Fig. 12. The T-H diagram of the ADWC-FP process

Fig. 12 illustrates the T-H chart of the ADWC-FP process, where the red and black lines demonstrate the CCC and HCC, respectively. In the ADWC-FP process, Q_{LP} is the low pressure steam consumption of H1-H4 and Q_{CW} indicates the cooling water requirements of coolers 1-3. From Fig. 12, the overlap region (green zone) is small between lines of HCC and CCC indicating that heat recovery is small. The low pressure steam and the cooling water requirements of the ADWC-FP process are 3045.4 and 3130.63 kW, respectively. In addition, 158.33 kW can be recovered by the observation of the heat recovery zone.

From the observation T-H diagram of Fig. 12, a lot of utilities are required in the ADWC-FP with preheated feed. All because, the 2982.5 kW of condenser (i.e., cooler 1) has been not effective utilized in the ADWC-FP process (Fig. 11). To effectively utilize the heat duty of the condenser and reduce the energy consumption of reboilers, HP technique is promising in saving cost of ADWC-FP systems. The applications of HP, a gas preheater for the compressor, and HEN to the ADWC-FP process are further investigated to improve the released heat duty quality of the condenser to meet the heat demand of the reboiler and reduce the cost.

3.2.2 Heat pump assisted ADWC (HP-ADWC2)

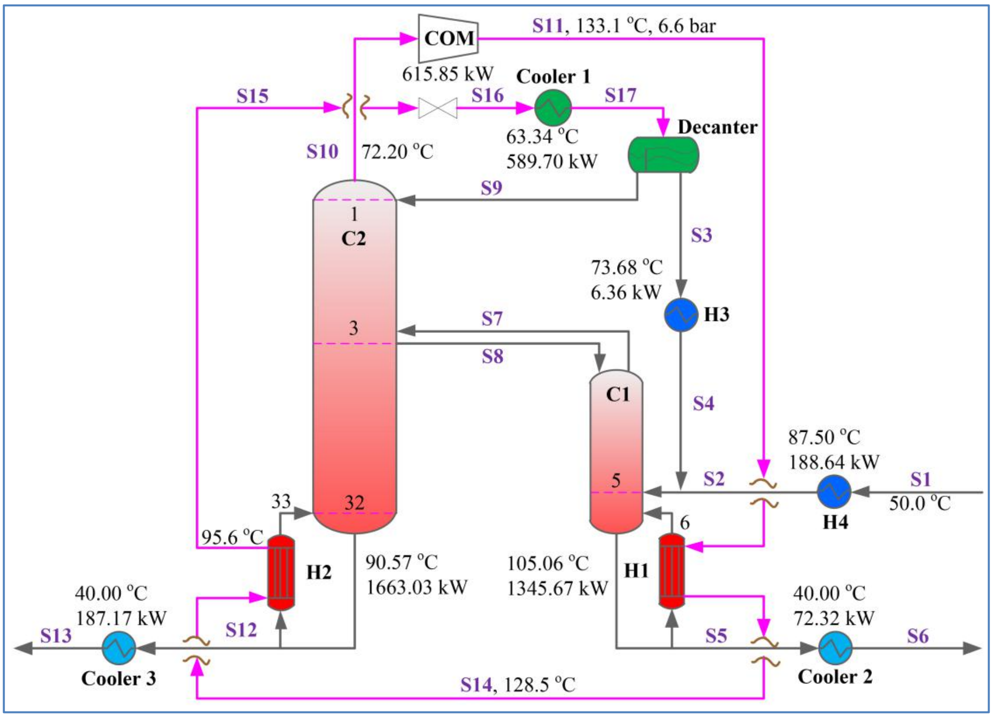

Fig. 13. Flowsheet of the proposed HP-ADWC2 process

Flowsheet of the proposed HP-ADWC2 process with detailed information to separate TBA/water system using entrainer CYH is demonstrated in Fig. 13. The top vapor stream of the column C2 is compressed to a higher temperature by a compressor (COM). The compressed stream can provide the duty to the reboiler of the columns C1 (H1) and then give the duty to the reboiler of the column C2 (H2). Finally, its pressure can be reduced by a valve and then is cooled by the cooler 1.

Temperature of the stream S15 (i.e., 95.6 °C) is lower than the saturated vapor temperature. Hence, a large compressor power 615.85 kW is required to achieve the heat exchange for H1 and H2. Following the suggestion in Section 2.2.3, TAC of the HP-ADWC2 may be reduced by increasing the temperature of compressor inlet (reducing the compressor power).

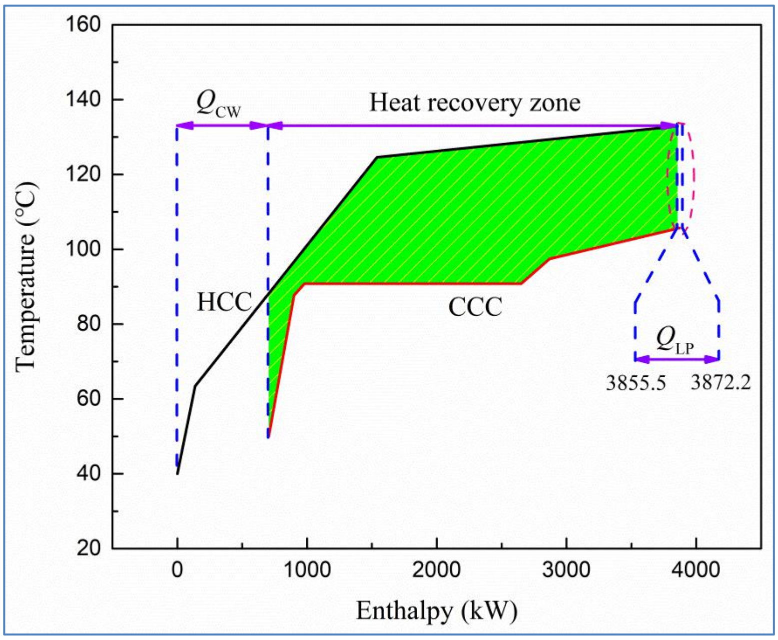

Fig. 14. T-H diagram of the HP-ADWC2 process

As is evident in Fig. 14, Q_{LP} and Q_{CW} of the HP-ADWC2 scheme are 16.7 kW and 705.00 kW, respectively. In addition, 3167.22 kW can be recovered by observation of the heat recovery zone. On the basic of above analysis, the HP-ADWC2 process can save much more energy compared to the ADWC-FP process. However, a larger compressor power is needed to improve the energy quality. As such, a further energy-saving configuration should be proposed to effectively reduce the compressor power via the installation of a gas preheater.

3.2.3 Adding a gas preheater to the HP-ADWC (GP-HP-ADWC)

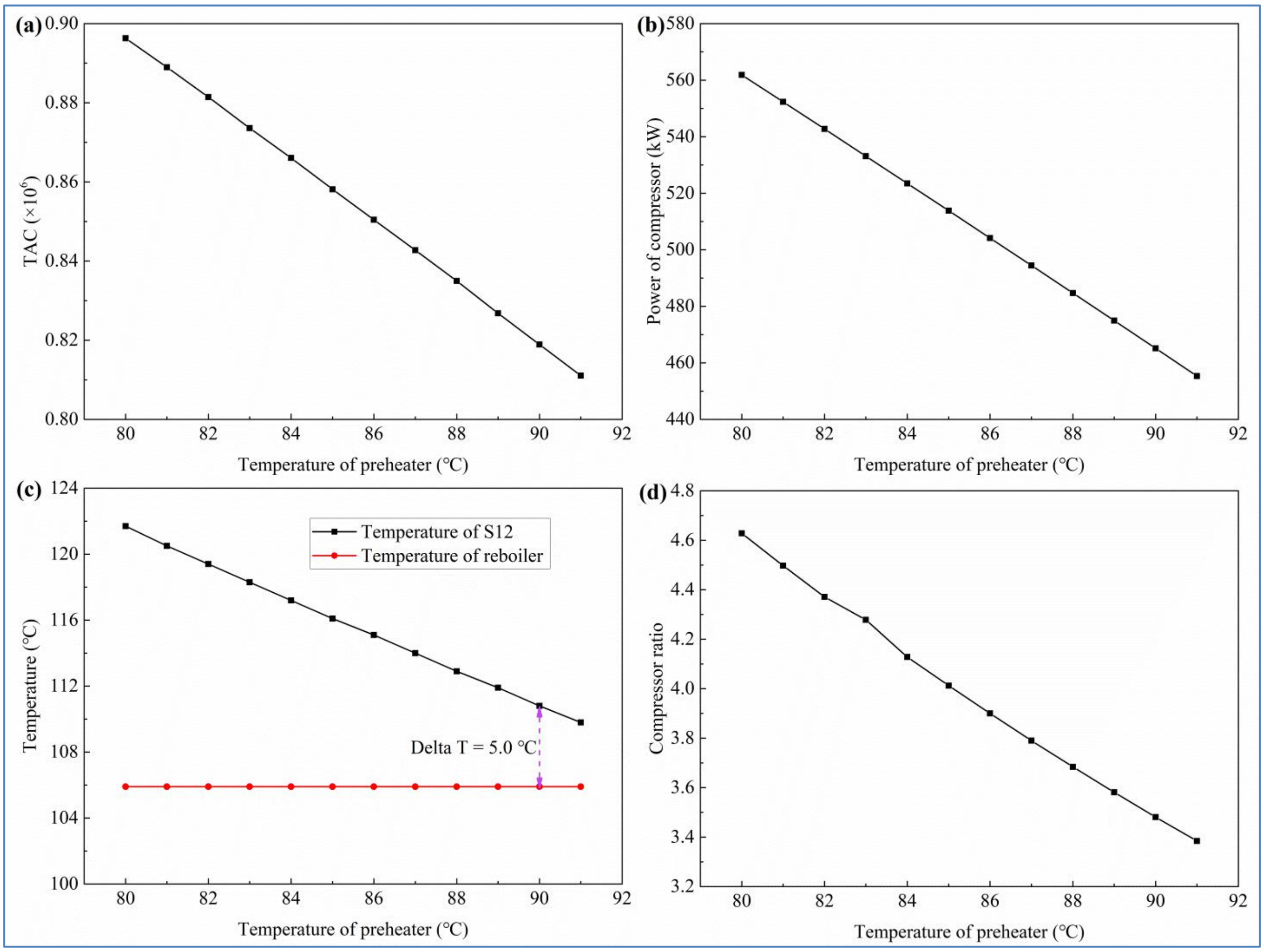

Fig. 15. Effect of temperature of preheater on (a) TAC, (b) power of compressor, (c) temperature of reboiler and preheater and (d) compressor ratio

From the Fig. 13, temperature of the recompressed stream by compressor is as usual high after heating the reboiler in the proposed HP-ADWC2 process. The energy is wasted directly when this stream enters the cooler 3. Consequently, HP system improvement is happening in the HP-ADWC2 to reduce the energy losses. A gas preheater before the compressor is installed in the HP-ADWC2 process (denoted as GP-HP-ADWC) to effectively reduce the energy consumption of the compressor. Fig. 15 demonstrates the effect of temperature of preheater on TAC, power of compressor, temperature of reboiler and preheater and compressor ratio. The results show that the temperature of preheater is determined as 89.9 ^{o}C to provide adequate temperature difference (Delta T) for reboiler H1.

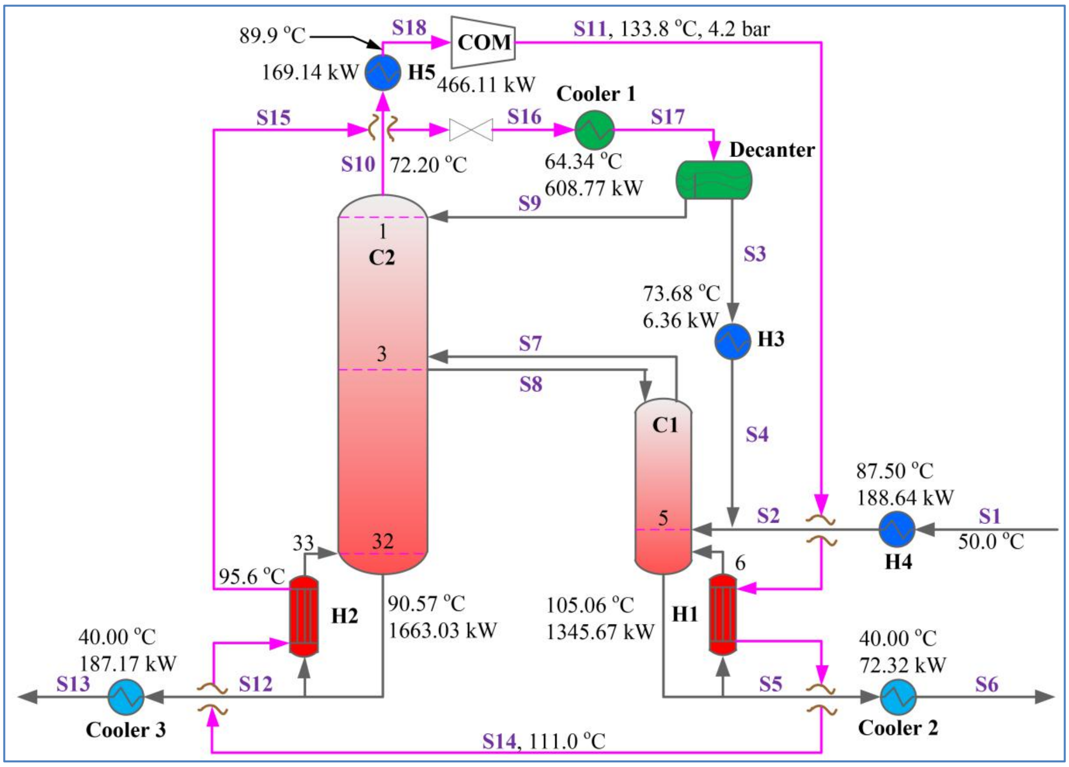

Fig. 16. Flowsheet of the GP-HP-ADWC process

Fig. 16 shows the GP-HP-ADWC process for separating TBA/water system with CYH as an entrainer. A gas preheater before the compressor is added to heat the vapor stream from the C2. Preheated vapor stream is then fed to the compressor achieving a higher temperature to provide heat duty for the two reboilers (H1 and H2).

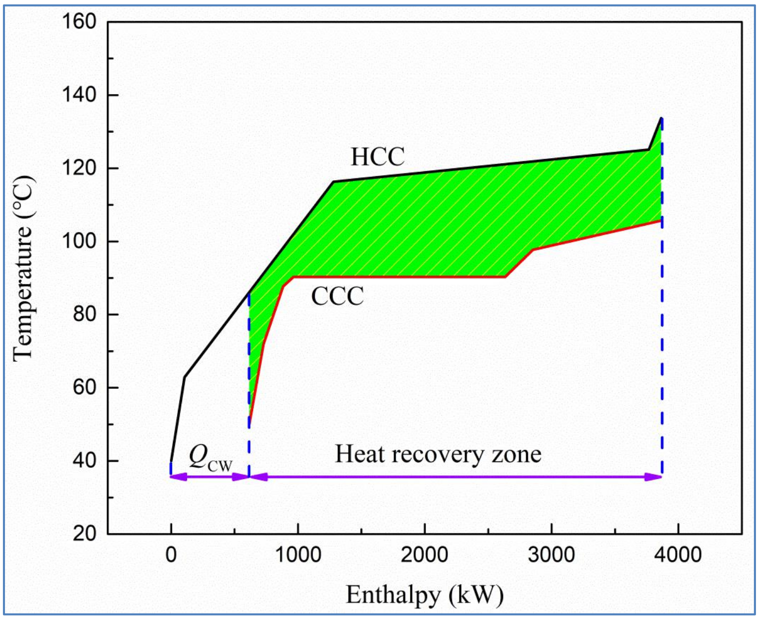

Fig. 17. T-H diagram of the GP-HP-ADWC process

As is depicted in Fig. 17, the cooling water demands of the GP-HP-ADWC design are 505.68 kW while no need additional steam in the GP-HP-ADWC process. Besides, 3248.06 kW can be recovered by the observation of the heat recovery zone (i.e., green region).

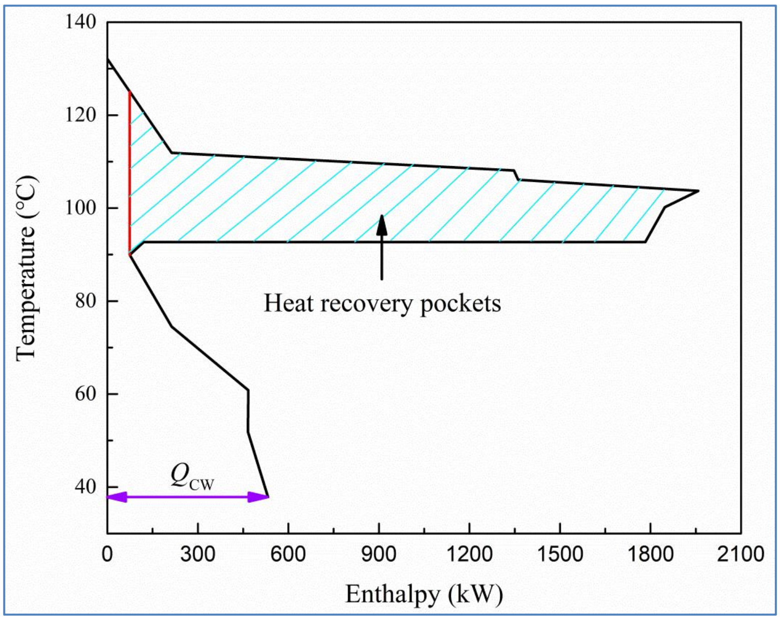

Fig. 18. Grand composition curve for the GP-HP-ADWC process

The heat recovery and utility demands at each temperature of the GP-HP-ADWC process could be analyzed via another effective tool grand composite curve (GCC). The minimum cooling water requirement Q_{CW} is the bottom residual of the GCC. Additionally, the wathet shaded area is heat recovery pockets where the heat can be circulated from hot streams to cold streams. Fig. 18 displays the GCC of the GP-HP-ADWC process. Obviously, there is no need to provide steam for the GP-HP-ADWC configuration. The minimum cooling requirements Q_{CW} in this process is 505.68 kW.

3.2.4 Self-heat ADWC (SH-ADWC) process

The large amount of superheat energy is observed via the T-H and GCC diagrams of GP-HP-ADWC process when the HP technology is used. Hence, the self-heat ADWC (SH-ADWC) is proposed based on the GP-HP-ADWC process to fully utilize the superheat energy. To design an energy-saving SH-ADWC process, the heat exchanger network (abbreviated as HEN) is an effective tool (Kim et al., 2009; Liu et al., 2018).

Table 3

Thermodynamic data for hot and cold streams in the GP-HP-ADWC process.

Stream	Stream type	T_{inlet} (°C)	T_{outlet} (°C)	Heat duty (kW)
To H1@C1_To_S5	Cold	87.8	105.9	1345.67
To H2@C2_To_S12	Cold	90.5	90.6	1663.03
S10_To_S18	Cold	72.2	89.9	169.14
S1_To_S2	Cold	50.0	87.5	188.64
S3_To_S4	Cold	67.4	73.7	6.36
S11_To_S17	Hot	133.8	63.3	3618.88
S5_To_S6	Hot	105.9	40.0	72.32
S12_To_S13	Hot	90.6	40.0	187.17

All detailed information of the hot and cold streams in the GP-HP-ADWC process are presented in Table 3. Hence, the minimum heat transfer temperature difference 5 °C is determined to achieve the minimum TAC, which is obtained by the Aspen Energy Analyzer.

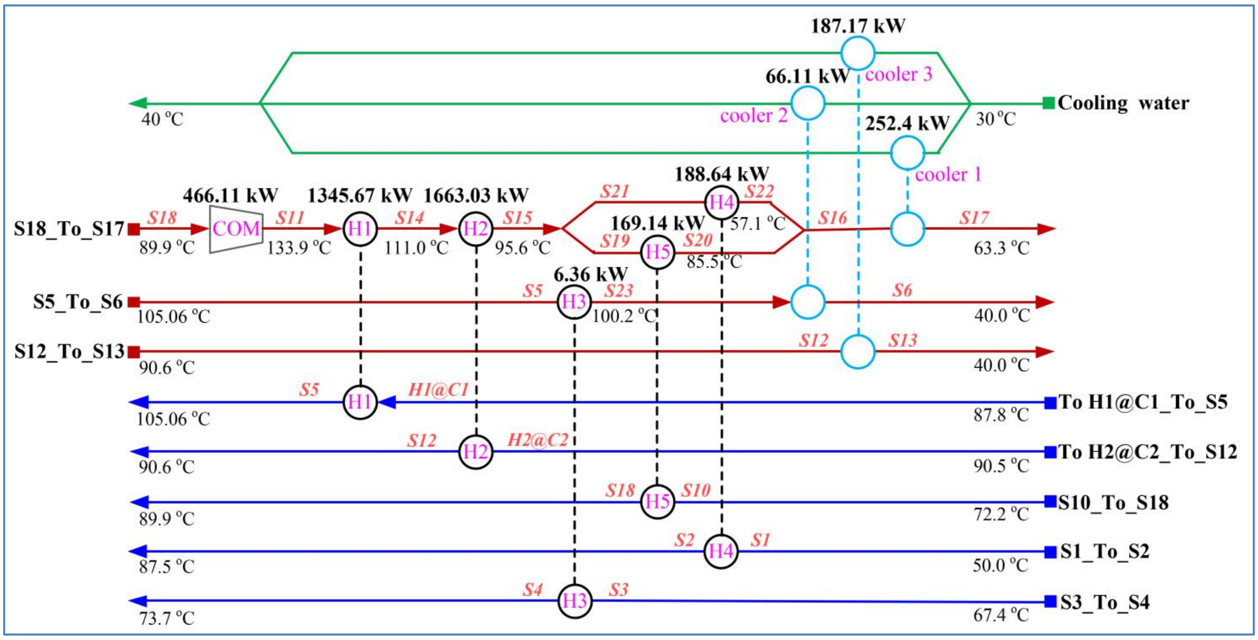

Fig. 19. Heat exchanger network for the SH-ADWC process

The optimal HEN of the GP-HP-ADWC process with eight heat exchangers is presented in Fig. 19. Among eight heat exchangers, heaters H1-H5 are self-heat exchangers, coolers 1-3 are coolers by using cooling water. The heating demand in the HEN is not needed while the cooling duty of only 505.68 kW is needed.

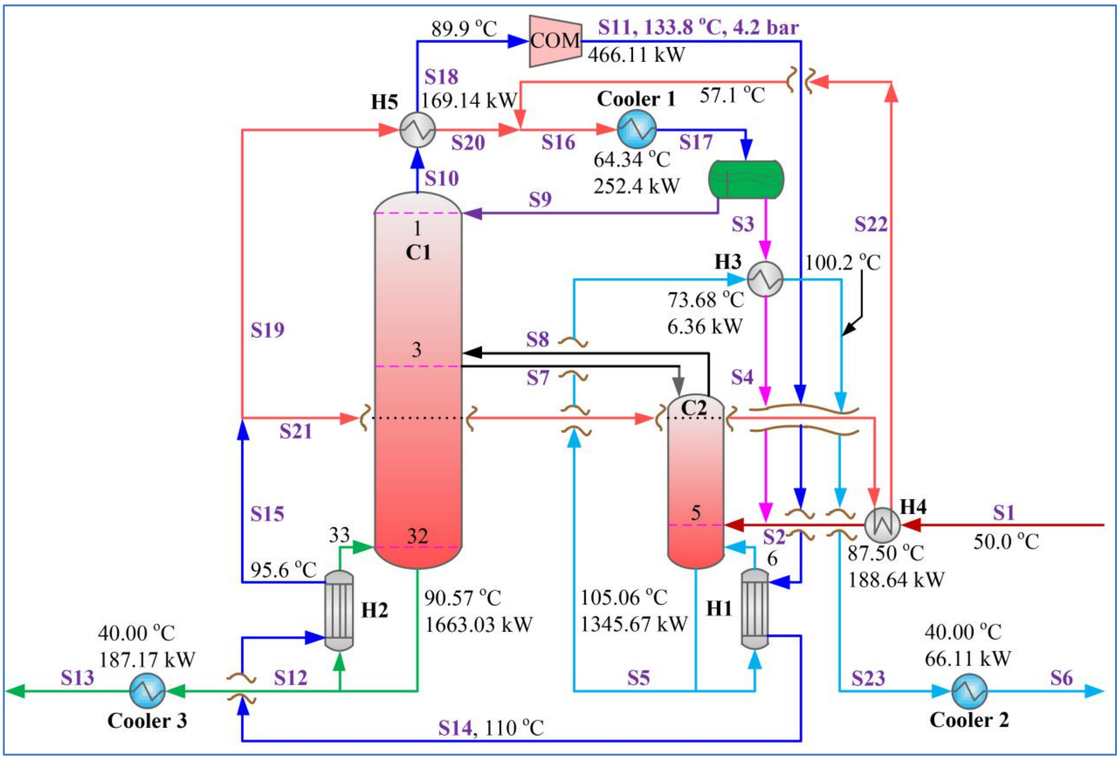

Fig. 20. Flowsheet of the proposed sustainable SH-ADWC process

The final process combined with the optimal HEN is illustrated in Fig. 20. In this work, electric power of 466.44 kW is needed to achieve the self-heating. The reboilers H1 and H2 are heated by the compressed streams S11 and S14, respectively. Additionally, the sensible heat of the streams S19 and S21 can be used to provide the heat duty of H5 and H4, respectively. The stream S3 is heated by the stream S5 (i.e., heat exchanger H3). Finally, cooling water is used in coolers 1-3 to cool the S16, S23, and S12 streams.

3.3 Performance evaluations

3.3.1 Economic evaluation

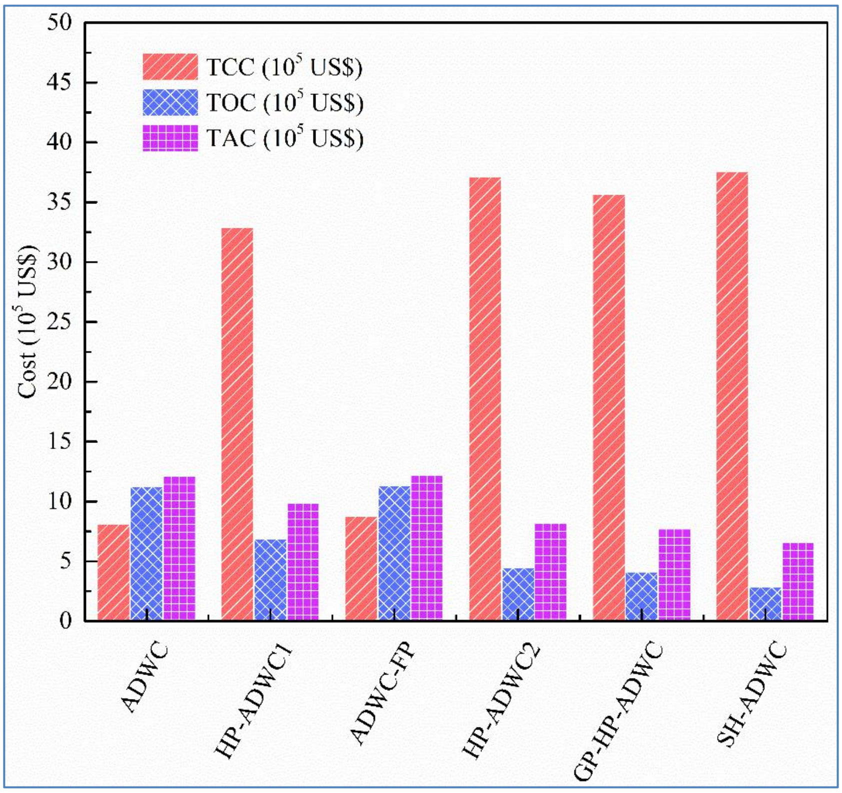

Figure 21. Economic comparisons of ADWC, HP-ADWC1, ADWC-FP, HP-ADWC2, GP-HP-ADWC and SH-ADWC processes

The economic comparisons between the four proposed designs and the two existing processes are summarized in Table A1 and Fig. 21. It is obvious that the capital cost of the HP assisted ADWC schemes (HP-ADWC1, HP-ADWC2, GP-HP-ADWC, and SH-ADWC) are higher than that of the ADWC processes (ADWC and ADWC-FP) because the capital cost of the compressor is expensive. However, TAC involves the energy and capital investments. The application of compressor makes full use of the latent and sensible heat of the compressed and product streams to provide the heat for reboiler and preheater, leading to reduce the operating cost of HP assisted ADWC schemes. Compared with the existing HP-ADWC1 design, the intensified SH-ADWC scheme can save 56.51% of TOC. Compared with the existing HP-ADWC1 scheme, TAC of the SH-ADWC process can save 32.91% with ten years payback period.

In addition, the total capital cost of the extractive distillation by Lo and Chien (2017) is

8.043×10^5 US$ and the re-calculation total operating cost is 7.870×10^5 US$. Hence, the total annual cost is 8.674×10^5 US$ with ten years payback period, which is far greater than the 6.624×10^5 US$ of the proposed SH-ADWC process.

Table A2 gives the comparison of the TNRs of the existing and proposed designs. TNRs of tert-butanol dehydration process are 146.077, 150.426, 145.955, 150.836, 152.366, and 153.629×10^5 US$ for ADWC, HP-ADWC1, ADWC-FP, HP-ADWC2, GP-HP-ADWC, and SH-ADWC schemes, respectively. TNR of the SH-ADWC process is 2.13% and 5.17% higher, respectively, compared to the existing ADWC and HP-ADWC1 processes.

3.3.2 Environmental evaluation

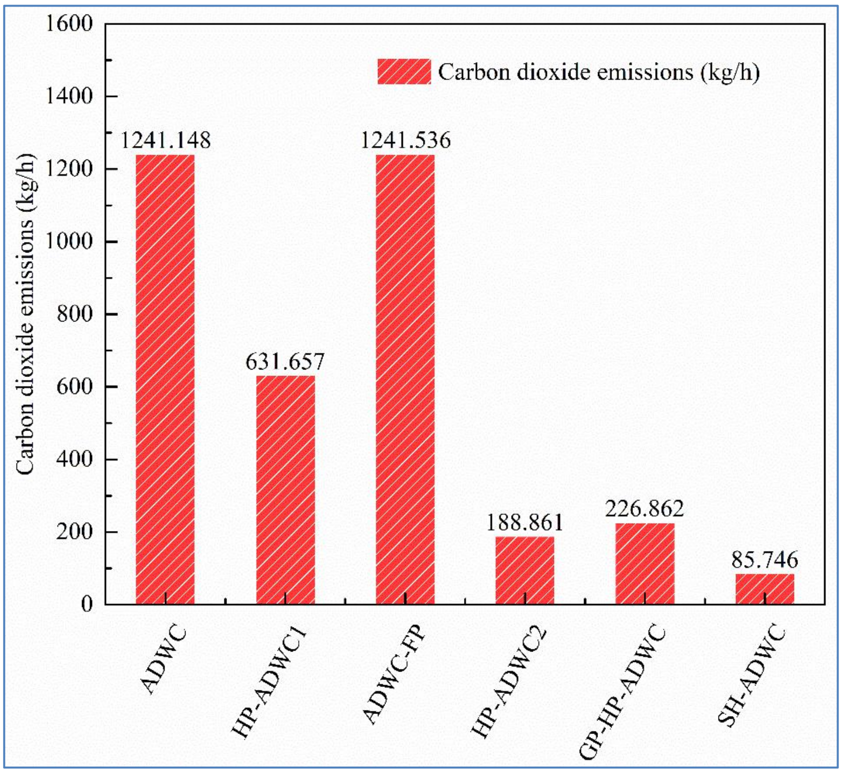

Fig. 22. Environmental comparisons of ADWC, HP-ADWC1, ADWC-FP, HP-ADWC2, GP-HP-ADWC and SH-ADWC processes

The CO_2 emissions of the ADWC, HP-ADWC1, ADWC-FP, HP-ADWC2, GP-HP-ADWC and SH-ADWC processes are 1241.148 kg/h, 631.657 kg/h, 1241.536 kg/h, 188.861 kg/h, 226.862 kg/h and 85.746 kg/h, respectively (see Fig. 22 and Table A3). Compared with the existing HP-ADWC1 process, the CO_2 emissions of the proposed HP-ADWC2, GP-HP-ADWC and SH-ADWC processes are reduced by 70.10%, 64.08% and 86.43%, respectively. Thus, the proposed intensified SH-ADWC scheme shows advantages in the reduction of CO_2 emissions.

3.3.3 Thermodynamic efficiency evaluation

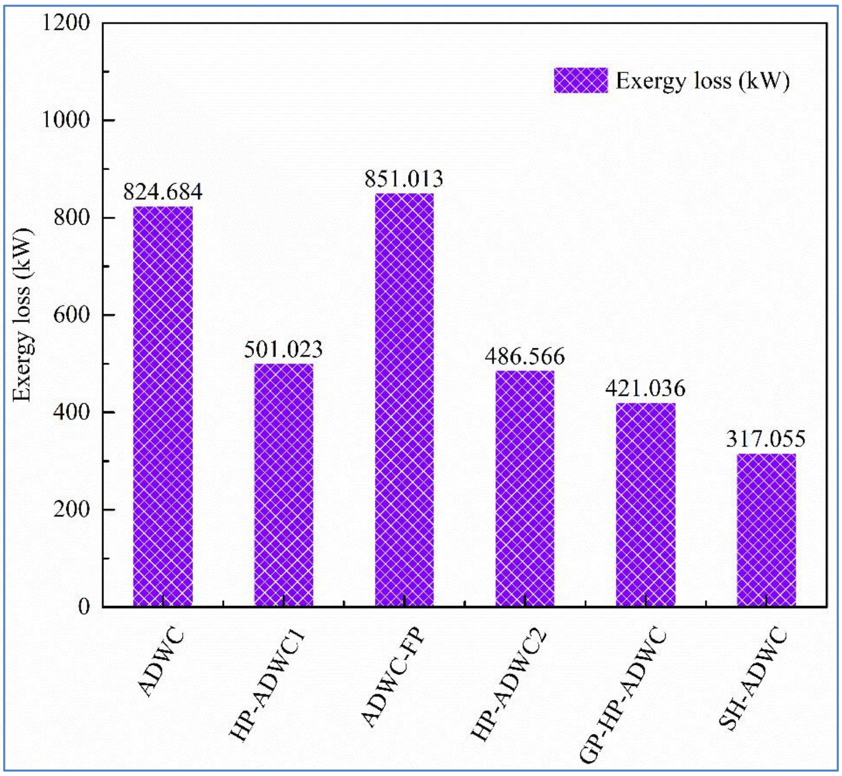

Fig. 23. Exergy loss comparisons of the existing and proposed processes

The exergy loss of the existing and four proposed processes is illustrated in Fig. 23 and Table A4. It indicates that the exergy loss of the existing processes and four proposed processes are 824.684 kW, 501.023 kW, 851.013 kW, 486.566 kW, 421.036 kW and 317.055 kW, respectively. Compared with the existing HP-ADWC1 process, the exergy loss of the SH-ADWC process is reduced by 36.72%.

In summary, the proposed SH-ADWC scheme is demonstrated to be more attractive in green and sustainable from the comparison on economic, thermodynamic, and environmental performances.

4. Conclusion

Herein, a novel green and sustainable self-heat azeotropic dividing wall column (SH-ADWC) scheme for separating azeotropic mixtures tert-butanol/water is proposed to achieve the performance of energy-saving, reduction of carbon dioxide emissions and enhancing of thermodynamic efficiency. The temperature-enthalpy and grand composite curve diagrams are used to analyze the energy consumption of the proposed configurations. Furthermore, the heat exchange network is utilized to design the optimal heat matching of the SH-ADWC process. ADWC-FP, HP-ADWC2 and GP-HP-ADWC processes are also designed to compare the economic, environmental and thermodynamic performances. The results demonstrate that total energy investment of the SH-ADWC scheme can be reduced by 56.51% compared with the HP-ADWC1 configuration. However, total capital investment of the SH-ADWC scheme is increased with the compressor is installed. The SH-ADWC process can save 32.91% of total annual cost (TAC) compared with the HP-ADWC1 scheme when the payback period is set as ten-year. The exergy loss of the proposed process is reduced by 36.72% compared with the existing HP-ADWC1 process by Luyben (2016). Moreover, it is found that the CO_2 emissions of the proposed SH-ADWC configuration can reduce 86.43% compared with the existing HP-ADWC1 process. As a consequence, the proposed green and sustainable SH-ADWC process show promising not only on TAC but also significantly reduces the exergy loss.

It is worth mentioning that there are three constraints needs to be considered when applying the proposed SH-ADWC configuration. Firstly, the temperature difference between the condenser and reboiler should be lower than 30 K or COP of the column exceeds 10. Secondly, the difference in heat duty between reboiler and condenser should be small enough. Thirdly, it should be the case that the amount of waste heat is not fully utilized.

Once the above constraints are met, the proposed method for the SH-ADWC configuration could be widely extended to other processes such as azeotropic, reactive, and extractive dividing wall column to effectively utilize the heat duty of condenser achieving reduction in TAC and sustainable development.

Appendix A. Supplementary data

Supplementary data to this article can be found online.

Acknowledgements:

This work was financially supported by the National Natural Science Foundation of China (Nos. 21878028 and 21606026 to W.S.; No. 21808117 to C.P.); the Chongqing Research Program of Basic Research and Frontier Technology (No. CSTC2016JCYJA0474 to W.S.). Helpful comments and suggestions from the paper's reviewers and editor are also gratefully acknowledged.

Notes

The authors declare no competing financial interest.

References:

Chen, J., Ye, Q., Liu, T., Xia, H., Feng, S., 2019. Improving the performance of heterogeneous azeotropic distillation via self-heat recuperation technology. Chem. Eng. Res. Des. 141, 516-528.

Douglas, J.M., 1988. Conceptual design of chemical processes. McGraw-Hill New York.

Feng, Z., Shen, W., Rangaiah, G.P., Lv, L., Dong, L., 2018. Process Development, Assessment, and Control of Reactive Dividing-Wall Column with Vapor Recompression for Producing n-Propyl Acetate. Ind. Eng. Chem. Res. 58(1), 276-295.

Gadalla, M., Olujic, Z., Derijke, A., Jansens, P., 2006. Reducing CO2 emissions of internally heat-integrated distillation columns for separation of close boiling mixtures. Energy 31(13), 2409-2417.

Gu, J., You, X., Tao, C., Li, J., Shen, W., Li, J., 2018. Improved design and optimization for separating tetrahydrofuran–water azeotrope through extractive distillation with and without heat integration by varying pressure. Chem. Eng. Res. Des. 133, 303-313.

Kim, J., Kim, J., Kim, J., Yoo, C., Moon, I., 2009. A simultaneous optimization approach for the design of wastewater and heat exchange networks based on cost estimation. J. Clean. Prod. 17(2), 162-171.

Kiss, A.A., Ignat, R.M., 2012. Enhanced methanol recovery and glycerol separation in biodiesel production – DWC makes it happen. Appl. Energy 99, 146-153.

Klemeš, J.J., Varbanov, P.S., Walmsley, T.G., Jia, X., 2018. New directions in the implementation of Pinch Methodology (PM). Renew. Sust. Energy Rev. 98, 439-468.

Kumar, V., Kiran, B., Jana, A.K., Samanta, A.N., 2013. A novel multistage vapor recompression reactive distillation system with intermediate reboilers. AIChE J. 59(3), 761-771.

Lei, Z., Yang, Y., Li, Q., Chen, B., 2009. Catalytic distillation for the synthesis of tert-butyl alcohol with structured catalytic packing. Catal. Today 147, S352-S356.

Li, R., Ye, Q., Suo, X., Dai, X., Yu, H., Feng, S., Xia, H., 2016. Improving the Performance of Heat Pump-Assisted Azeotropic Dividing Wall Distillation. Ind. Eng. Chem. Res. 55(22), 6454-6464.

Liu, J., Yang, Y., Wei, S.a., Shen, W., Rakovitis, N., Li, J., 2018. Intensified p-Xylene Production Process through Toluene and Methanol Alkylation. Ind. Eng. Chem. Res. 57(38), 12829-12841.

Lo, K.-M., Chien, I.L., 2017. Efficient separation method for tert-butanol dehydration via extractive distillation. J. Taiwan Inst. Chem. E. 73, 27-36.

Long, N.V.D., Minh, L.Q., Nhien, L.C., Lee, M., 2015. A novel self-heat recuperative dividing wall column to maximize energy efficiency and column throughput in retrofitting and debottlenecking of a side stream column. Appl. Energy 159, 28-38.

Luo, H., Bildea, C.S., Kiss, A.A., 2015. Novel Heat-Pump-Assisted Extractive Distillation for Bioethanol Purification. Ind. Eng. Chem. Res. 54(7), 2208-2213.

Luyben, W.L., 2012. Principles and case studies of simultaneous design. John Wiley & Sons.

Luyben, W.L., 2016. Control of an azeotropic DWC with vapor recompression. Chem. Eng. Process 109, 114-124.

Luyben, W.L., Chien, I.-L., 2011. Design and control of distillation systems for separating azeotropes. John Wiley & Sons.

Matsuda, K., Kansha, Y., Fushimi, C., Tsutsumi, A., Kishimoto, A., 2012. Advanced energy saving and its applications in industry. Springer Science & Business Media.

Modla, G., Lang, P., 2013. Heat pump systems with mechanical compression for batch distillation. Energy 62, 403-417.

Modla, G., Lang, P., 2015. Vapor Compression for Batch Distillation: Comparison of Different Working Fluids. Ind. Eng. Chem. Res. 54(3), 1081-1092.

Olujić, Ž., Sun, L., de Rijke, A., Jansens, P.J., 2006. Conceptual design of an internally heat integrated propylene-propane splitter. Energy 31(15), 3083-3096.

Pleşu, V., Ruiz, A.E.B., Bonet, J., Llorens, J., 2014. Simple Equation for Suitability of Heat Pump Use in Distillation. Comput. Aided Process Eng. 33, 1327-1332.

Poddar, T., Jagannath, A., Almansoori, A., 2017. Use of reactive distillation in biodiesel production:

A simulation-based comparison of energy requirements and profitability indicators. Appl. Energy 185, 985-997.

Premkumar, R., Rangaiah, G.P., 2009. Retrofitting conventional column systems to dividing-Wall Columns. Chem. Eng. Res. Des. 87(1), 47-60.

PHC, 2016. https://www.pharmacompass.com/price/tert-butanol

Santaella, M.A., Jiménez, L.E., Orjuela, A., Segovia-Hernández, J.G., 2017. Design of thermally coupled reactive distillation schemes for triethyl citrate production using economic and controllability criteria. Chem. Eng. J. 328, 368-381.

Sharan, P., Neises, T., Turchi, C., 2018. Optimal feed flow sequence for multi-effect distillation system integrated with supercritical carbon dioxide Brayton cycle for seawater desalination. J. Clean. Prod. 196, 889-901.

Silva, R.O., Torres, C.M., Bonfim-Rocha, L., Lima, O.C.M., Coutu, A., Jiménez, L., Jorge, L.M.M., 2018. Multi-objective optimization of an industrial ethanol distillation system for vinasse reduction – A case study. J. Clean. Prod. 183, 956-963.

Silva, W.C., Araújo, E.C.C., Calmanovici, C.E., Bernardo, A., Giulietti, M., 2017. Environmental assessment of a standard distillery using aspen plus®: Simulation and renewability analysis. J. Clean. Prod. 162, 1442-1454.

Sun, X., Wu, J., Wang, R., 2013. Exergy analysis and comparison of multi-functional heat pump and conventional heat pump systems. Energy Convers. Manage. 73, 51-56.

Tavan, Y., Shahhosseini, S., Hosseini, S.H., 2014. Design and simulation of ethane recovery process in an extractive dividing wall column. J. Clean. Prod. 72, 222-229.

Todd, R., Baroutian, S., 2017. A techno-economic comparison of subcritical water, supercritical

CO2 and organic solvent extraction of bioactives from grape marc. J. Clean. Prod. 158, 349-358.

Turton, R., Bailie, R.C., Whiting, W.B., Shaeiwitz, J.A., 2008. Analysis, synthesis and design of chemical processes. Pearson Education.

Tututi-Avila, S., Medina-Herrera, N., Hahn, J., Jiménez-Gutiérrez, A., 2017. Design of an energy-efficient side-stream extractive distillation system. Comput. Chem. Eng. 102, 17-25.

Waheed, M.A., Oni, A.O., Adejuyigbe, S.B., Adewumi, B.A., Fadare, D.A., 2014. Performance enhancement of vapor recompression heat pump. Appl. Energy 114, 69-79.

Walmsley, T.G., Lal, N.S., Varbanov, P.S., Klemeš, J.J., 2018. Automated retrofit targeting of heat exchanger networks. Front. Chem. Sci. Eng. 12(4), 630-642.

Wang, C., Guang, C., Cui, Y., Wang, C., Zhang, Z., 2018. Compared novel thermally coupled extractive distillation sequences for separating multi-azeotropic mixture of acetonitrile/benzene/methanol. Chem. Eng. Res. Des. 136, 513-528.

Wang, Y., Bu, G., Geng, X., Zhu, Z., Cui, P., Liao, Z., 2019a. Design optimization and operating pressure effects in the separation of acetonitrile/methanol/water mixture by ternary extractive distillation. J. Clean. Prod. 218, 212-224.

Wang, Y., Feng, X., Cai, Y., Zhu, M., Chu, K.H., 2009. Improving a process's efficiency by exploiting heat pockets in its heat exchange network. Energy 34(11), 1925-1932.

Wang, Y., Liu, X., Kraslawski, A., Gao, J., Cui, P., 2019b. A novel process design for CO_2 capture and H_2S removal from the syngas using ionic liquid. J. Clean. Prod. 213, 480-490.

Wu, Y.C., Hsu, P.H.-C., Chien, I.L., 2013. Critical Assessment of the Energy-Saving Potential of an Extractive Dividing-Wall Column. Ind. Eng. Chem. Res. 52(15), 5384-5399.

Wu, Y.C., Lee, H.-Y., Huang, H.-P., Chien, I.L., 2014. Energy-Saving Dividing-Wall Column

Design and Control for Heterogeneous Azeotropic Distillation Systems. Ind. Eng. Chem. Res. 53(4), 1537-1552.

Xia, H., Ye, Q., Feng, S., Li, R., Suo, X., 2017. A novel energy-saving pressure swing distillation process based on self-heat recuperation technology. Energy 141, 770-781.

Xie, Q., Cai, L., Xia, F., Liang, X., Wu, Z., Liu, Y., Li, X., Lu, M., Nie, Y., Ji, J., 2019. High vacuum distillation for low-sulfur biodiesel production: From laboratory to large scale. J. Clean. Prod. 223, 379-385.

Xu, L., Li, M., Ge, X., Yuan, X., 2017. Numerical simulation of dividing wall column with vapor recompression located at side product stage. Chem. Eng. Res. Des. 120, 138-149.

Yang, A., Lv, L., Shen, W., Dong, L., Li, J., Xiao, X., 2017. Optimal Design and Effective Control of the tert-Amyl Methyl Ether Production Process Using an Integrated Reactive Dividing Wall and Pressure Swing Columns. Ind. Eng. Chem. Res. 56(49), 14565-14581.

Yang, A., Shen, W., Wei, S.a., Dong, L., Li, J., Gerbaud, V., 2019a. Design and control of pressure-swing distillation for separating ternary systems with three binary minimum azeotropes. AIChE J. 65(4), 1281-1293.

Yang, A., Sun, S., Eslamimanesh, A., Wei, S.a., Shen, W., 2019b. Energy-saving investigation for diethyl carbonate synthesis through the reactive dividing wall column combining the vapor recompression heat pump or different pressure thermally coupled technique. Energy 172, 320-332.

Yang, A., Wei, R., Sun, S., Wei, S.a., Shen, W., Chien, I.L., 2018. Energy-Saving Optimal Design and Effective Control of Heat Integration-Extractive Dividing Wall Column for Separating Heterogeneous Mixture Methanol/Toluene/Water with Multiazeotropes. Ind. Eng. Chem. Res. 57(23), 8036-8056.

Yang, M., Feng, X., Liu, G., 2016. Heat integration of heat pump assisted distillation into the overall process. Appl. Energy 162, 1-10.

You, X., Gu, J., Peng, C., Shen, W., Liu, H., 2017. Improved Design and Optimization for Separating Azeotropes with Heavy Component as Distillate through Energy-Saving Extractive Distillation by Varying Pressure. Ind. Eng. Chem. Res. 56(32), 9156-9166.

You, X., Rodriguez-Donis, I., Gerbaud, V., 2016. Reducing process cost and CO2 emissions for extractive distillation by double-effect heat integration and mechanical heat pump. Appl. Energy 166, 128-140.

Yu, H., Ye, Q., Xu, H., Zhang, H., Dai, X., 2015. Design and Control of Dividing-Wall Column for tert-Butanol Dehydration System via Heterogeneous Azeotropic Distillation. Ind. Eng. Chem. Res. 54(13), 3384-3397.

Zhao, Y., Ma, K., Bai, W., Du, D., Zhu, Z., Wang, Y., Gao, J., 2018. Energy-saving thermally coupled ternary extractive distillation process by combining with mixed entrainer for separating ternary mixture containing bioethanol. Energy 148, 296-308.

Zhou, H., Cai, Y., You, F., 2018. Systems Design, Modeling, and Thermoeconomic Analysis of Azeotropic Distillation Processes for Organic Waste Treatment and Recovery in Nylon Plants. Ind. Eng. Chem. Res. 57(30), 9994-10010.